



A comparative study of the common persulfate activation techniques for the complete degradation of an NSAID: The case of ketoprofen



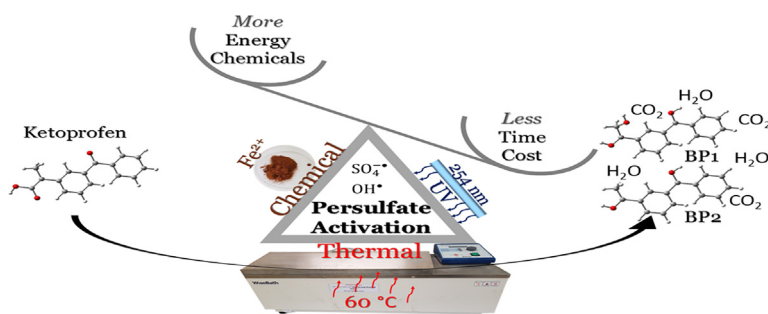
Maya Amasha, Abbas Baalbaki, Antoine Ghauch*

American University of Beirut, Faculty of Arts and Sciences, Department of Chemistry, P.O. Box 11-0236, Riad El Solh, 1107-2020 Beirut, Lebanon

HIGHLIGHTS

- Rapid KTP mineralization is achieved in UV-activated PS system only.
- Direct photolysis contributes greatly to KTP degradation in UV-activated PS system.
- UV-activated PS system is effective in both KTP and partial bacterial removal.
- KTP degradation mechanism involves both $\text{SO}_4^{\cdot-}$ and OH^{\cdot} .
- Rapid KTP removal is cost effective in UV-activated PS system.

GRAPHICAL ABSTRACT



ARTICLE INFO

Keywords:

Ketoprofen
Persulfate
Heat
UV
 Fe^{2+}
Degradation

ABSTRACT

This work assessed the treatment of ketoprofen (KTP) using persulfate (PS) based Advanced Oxidation Process (AOP) activated thermally, chemically (Fe^{2+}) or by UV. KTP degradation was optimized by manipulating several experimental parameters to achieve efficient KTP and its byproducts removal. Parameters included: PS concentration, Fe^{2+} concentration, temperature, pH, dissolved ions e.g. Cl^- , HCO_3^- , and humic acids (HA). Results showed that: (i) KTP degraded significantly in UV only systems in contrary to thermal and chemical systems where KTP was resistant in PS free solutions; (ii) KTP degradation extent increased with the increase in $[\text{PS}]_0$ while it was highly dependent on the $[\text{Fe}^{2+}]_0: [\text{PS}]_0$ molar ratio; (iii) The activation energy (E_A) calculated in thermal activation experiments was found to be $157.02 (\pm 8.9) \text{ kJ mol}^{-1}$; (iv) The highest % reaction stoichiometric efficiency calculated only in thermal systems reached 38%; (v) Sequential KTP additions showed that the UV system was the most sustainable, followed by the thermal system while the chemical system was the least sustainable. (vi) KTP dissolved in a non-treated waste water matrix was best removed along with present coliforms in UV system. KTP transformation products were identified by HPLC/MS and a degradation reaction pathway was suggested. This study led to the conclusion that UV/PS systems are the most economically efficient among the three investigated PS-based systems.

1. Introduction

Non-steroidal anti-inflammatory drugs (NSAIDs) have been widely used in human medicine in the last few decades, especially that they are available over the counter, low in cost, and are characterized by the

absence of addictive side effects [1]. Pharmaceuticals in the aquatic environment were found to alter the physiological processes in fish, by binding to their nuclear receptors thus altering molecular mechanisms at the transcription and/or translation levels [2]. A recent study conducted in 2013 showed that NSAIDs caused adverse histopathological

* Corresponding author.

E-mail address: antoine.ghauch@aub.edu.lb (A. Ghauch).

<https://doi.org/10.1016/j.cej.2018.05.118>

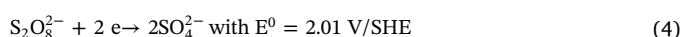
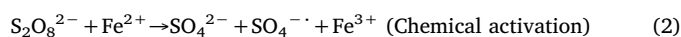
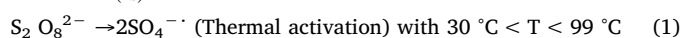
Received 22 March 2018; Received in revised form 17 May 2018; Accepted 20 May 2018
Available online 28 May 2018

1385-8947/ © 2018 Elsevier B.V. All rights reserved.

changes in various tissues of many species [3]. NSAIDs are delivered to several environmental compartments through different routes originating from various sources. Among the main routes of entry is domestic wastewater in which human excretions containing non-metabolized pharmaceuticals and improperly disposed medication find their way into sewage treatment plants (STPs) [4,5]. Other entry routes include the discharge from manufacturing sites, therapeutic treatment of livestock and effluents from aquaculture farms that were proven to significantly contribute to the environmental contamination by NSAIDs [6–10]. Conventional STPs are not effective in removing complex organic compounds such as NSAIDs; therefore, a substantial amount of these contaminants and their metabolites enter the aquatic environment and reach groundwater [5,11–14], and consequently have been found in surface, and drinking water [15–17]. Micropollutants such as pharmaceuticals can be subjected to sorption on sludge in primary WWTPs; however, the removal efficiency reached was rather low (28%) [18]. In secondary WWTPs, pharmaceuticals are subjected to several processes such as dispersion, dilution, partitioning, biodegradation and abiotic transformation [19]. NSAIDs particularly haven't exhibited effective removal extent in secondary WWTPs through biodegradation, where a maximum removal of 75% was reached in a very limited number of NSAIDs as reported by Selgado et al. [20]. Among the many NSAIDs detected in natural waters, ketoprofen (KTP) (Table 1S) is considered one of the most representative drugs of this class of pharmaceuticals which was found in concentrations up to $6 \mu\text{g L}^{-1}$ [21–24]. Several research groups investigated KTP removal using different biological and chemical methods. Nakada et al. [25] investigated KTP elimination in a municipal STP using activated sludge treatment; however, KTP showed poor removal (< 50%). Urrea et al. [26] studied KTP degradation by the aid of a white-rot fungus in a liquid medium where % degradation reached 100% after 24 h of treatment. On the other hand, many research groups aimed for degrading KTP chemically such as Fan et al. [27] who applied fabricated mesoporous Sb-doped SnO_2 electrode for the electrochemical degradation of KTP. A maximum of 70% TOC was removed upon treatment over a period of 4 h. Murgananthan et al. [28] also investigated KTP degradation using boron doped diamond (BDD) and platinum electrodes. KTP was fully degraded after a period of 2 h at a current density of 13.3 mA cm^{-2} ; however, TOC removal required 12 h of treatment using Na_2SO_4 as a supporting electrolyte. Feng et al. [29] found out that electro-Fenton process on a BDD electrode is a rapid method for KTP removal (30 min), while full mineralization expanded over a period of 4 h. Other research groups studied the photodegradation of KTP, alone or mixed with other pharmaceuticals where they were able to totally remove KTP; however, its degradation byproducts/TOC remaining persisted in the reaction mixture requiring longer exposure period [30–32]. KTP degradation was also studied under the effect of O_3 and UV/ O_3 systems where the latter was 14–15 times ($\approx 90\%$) more efficient towards KTP degradation and mineralization [33]. In addition, Hilles et al. [34] and Abu Amr et al. [35] investigated PS/ H_2O_2 and PS/ O_3 performance respectively. This was done for the treatment of stabilized leachate, showing increased efficiency when PS is combined with H_2O_2 or O_3 , which was confirmed by the improvement in COD removal in these systems compared to PS only system. On the other hand, a very recent work has been published by Feng et al. [36] on thermally activated PS (T-APS) for the degradation of ketoprofen, where KTP almost fully degraded (97%) under neutral conditions at $T = 50^\circ\text{C}$ and $[\text{PS}]_0 = 2 \text{ mM}$ after 2 h of reaction.

Activated PS has been extensively studied to be used in water and soil remediation as it reacts with a wide range of organic contaminants [37]. During the last decade, AOPs researchers developed PS technology by studying different activation techniques, interferences from naturally occurring mineral species, and efficiency and sustainability of PS over long treatment periods to optimize the oxidation reactions. The most common PS activation techniques are thermal (Eq. (1)) [38–40], chemical (Eq. (2)) [41,42], and UV (Eq. (3)) [43,44] activation alone or

combined. Upon activation, PS ($E^0 = 2.01 \text{ V}$) is transformed into sulfate radicals (SRs, $E^0 = 2.6 \text{ V}$) which are very reactive towards organic contaminants (OCs) due to their non-selectivity [37]. The number of SRs formed per PS molecule depends on the activation technique and are shown in Eqs. 1–3. The mode of action of SRs is mainly through electron abstraction, therefore it is extremely reactive towards contaminants containing non-bonding electron pairs on atoms such as S, N and O [37,45,46]. In the case of high abundance of SRs in the reaction medium, parasitic reactions could take place leading to less efficient contaminant degradation. These reactions are mainly attributed to the self-quenching of SRs in T-APS and UV activated PS systems (UV-APS), and to the metal-ion quenching in a chemically activated PS system (Fe-APS) [42,44]. Therefore, it is essential to optimize the reaction conditions to avoid any loss of energy and materials. These conditions can be determined by calculating the reaction stoichiometric efficiency (RSE) value, whenever applicable, which is defined as the number of moles of the target OC degraded versus the number of moles of PS consumed $\% \text{RSE} = \frac{\Delta n(\text{OC})}{\Delta n(\text{PS})} \times 100$.



To the best of our knowledge, degradation of KTP using PS in AOPs has never been investigated except for the lone study done by Feng et al. limited to T-APS [36]. Therefore, our aim in this work is to obtain a comprehensive comparative study on KTP degradation using the most common PS activation techniques: thermal, UV, and chemical activation under the scenario of the effluent of a pharmaceutical production facility. The study will also include the effect of several experimental variables such as pH, $[\text{PS}]_0$, inorganic ions (Cl^- , HCO_3^-), natural organic matter (NOM) specifically humic acids (HA), and natural water samples: wastewater (WW), sea water (SW), and spring water (SpW). The observed reaction rate constants (k_{obs}) obtained from all the mentioned experiments are compared to determine the most robust activation technique. Mineralization tests conducted using TOC analysis are obtained for the three activation methods while the % RSE values were determined whenever applicable. HPLC/MS was used to help elucidating the degradation pathways and mechanisms. Finally, an economic assessment of the three activation methods was done to identify the most economically efficient method for future applications.

2. Materials and methods

2.1. Chemicals

Ketoprofen ($\text{C}_{16}\text{H}_{14}\text{O}_3$), sodium persulfate (PS) ($\text{Na}_2\text{S}_2\text{O}_8$, $\geq 99.0\%$), phosphate buffer (monobasic and dibasic), humic acids and potassium iodide (KI) (puriss, 99.0–100.5%) were purchased from Sigma-Aldrich (China, France, Germany, Switzerland, and Germany, respectively). Iron (II) chloride tetrahydrate ($\text{FeCl}_2 \cdot 4\text{H}_2\text{O}$) (purum $\geq 98\%$) and hydrochloric acid (HCl) were acquired from Fluka (Switzerland and Netherlands, respectively). To assess the ionic additives effect, sodium chloride (NaCl) and sodium hydrogen carbonate (NaHCO_3) were purchased from Fluka (Netherlands). Formic acid used for the HPLC mobile phase was purchased from Loba Chemie (India). Millipore deionized water (DI) was used in the preparation of all solutions.

2.2. Chemical analysis

Methods of analysis of KTP, PS and TOC are provided in Supporting

Information (see text S1, Fig. 2S, 3S).

2.3. Chemical setup

Control experiments were performed either in the absence of PS or its activator (heat, UV, or Fe^{2+}). All KTP degradation experiments were done in duplicates and each sample was analyzed twice for uncertainty determination, $[\text{KTP}]_0$ was chosen to be 2 mg L^{-1} ($7.87 \mu\text{M}$) in all experiments done except for TOC and MS analysis where it was 10 mg L^{-1} ($39.35 \mu\text{M}$) for better sensitivity. The high initial $[\text{KTP}]_0 = 2 \text{ mg L}^{-1}$ was chosen to mimic wastewater from the effluent of a pharmaceutical production facility; accordingly, the $[\text{PS}]_0$, $[\text{Fe}^{2+}]_0$, temperature and UV intensity were all chosen in the functional range for real life treatment scenarios. It is worth noting that our research group already audited a Lebanese pharmaceutical production facility and screened its wastewater for pharmaceuticals; their concentration was in the mg L^{-1} level.

2.3.1. Thermal activation reactors

Experiments were done in 200 mL Erlenmeyer flasks placed in a temperature controlled ($\pm 1^\circ\text{C}$) water bath with the required temperature ($40\text{--}70^\circ\text{C}$) and shaking speed (80 rpm) preset. A complete schematic of the setup is shown in Fig. 1a.

2.3.2. Chemical activation reactors

Experiments were done in 200 mL Erlenmeyer flasks placed on stirring plates of a constant stirring speed (240 rpm) at room temperature (25°C). A complete schematic of the setup is shown in Fig. 1b.

2.3.3. UV activation reactors

Experiments were performed in 400 mL borosilicate reactors each fitted with a quartz insert and a commercial 6 W low-pressure mercury lamp (LpHgL). The LpHgLs exhibited an intensity of 2.3 mW/cm^2 at a radial distance of 3.00 cm as experimentally determined by a Radiometer measurement (Model UVC-254 Lutron; Taipei, Taiwan) which is the same distance between the lamp and the solution surface. The reactors were placed in a temperature-controlled water bath fixed

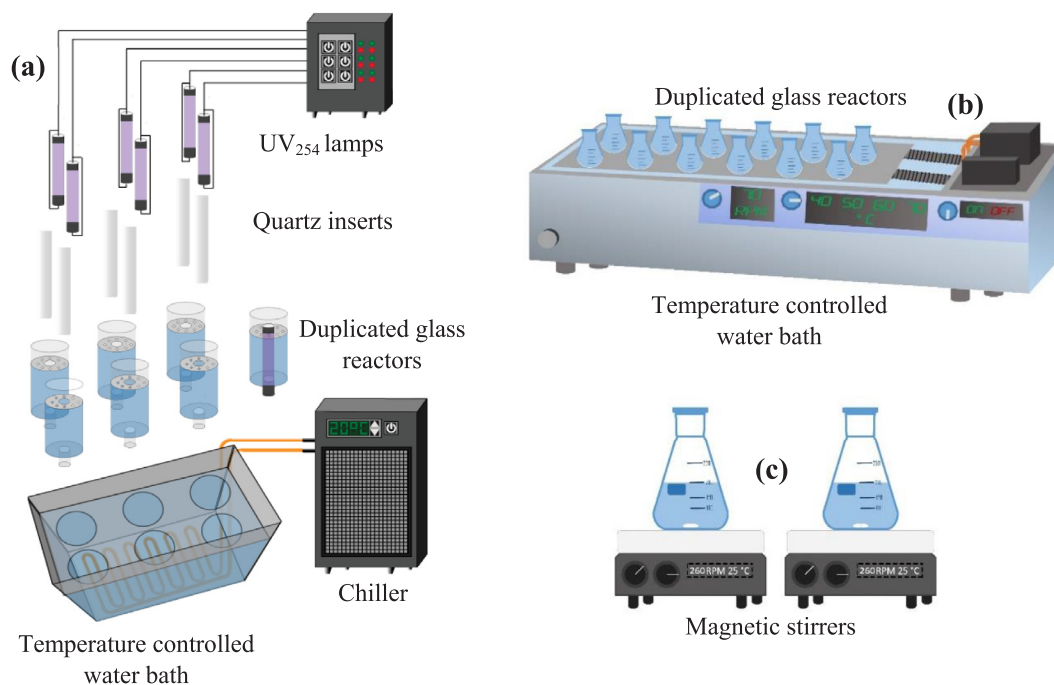


Fig. 1. Setup used for KTP degradation in (a) UV-APS, (b) T-APS, and (c) Fe-APS. Experiments were done in parallel under similar conditions for reproducibility measurements.

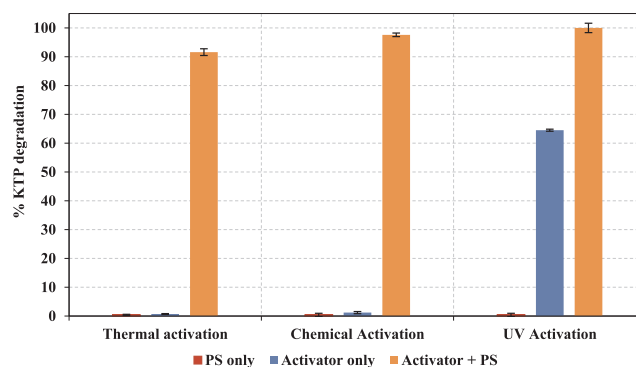


Fig. 2. % KTP degradation in “PS only”, “activator only” and “activator + PS” in the three activation systems. Experimental conditions: $[\text{KTP}]_0 = 7.87 \mu\text{M}$ in the three systems, $[\text{PS}]_0 = 1.0 \text{ mM}$ (T-APS), $[\text{PS}]_0 = 0.5 \text{ mM}$ and $[\text{Fe}^{2+}]_0 = 0.1 \text{ mM}$ (Fe-APS), $[\text{PS}]_0 = 0.1 \text{ mM}$ (UV-APS). $\text{pH}_{i(\text{avg})} = 6.15$, pH_f (T-APS) = 3.85, pH_f (Fe-APS) = 3.19, pH_f (UV-APS) = 5.92.

at $20 (\pm 1)^\circ\text{C}$. A complete schematic of the setup is shown in Fig. 1c.

2.3.4. Experimental procedure

Solution preparation, sampling and analysis conditions are provided in Supporting Information (see text S2).

3. Results and discussion

3.1. Optimization of experimental conditions for all activated PS systems

3.1.1. Control experiments: PS free vs. PS spiked systems

The degradation of KTP has been investigated in the presence and in the absence of PS as presented in Fig. 2. Reactions were performed over a period of 1 h in T-APS and Fe-APS, and 10 min in UV-APS. All reaction mixtures in the three systems were unbuffered except for the pH study which is presented in Section 3.3. It can be clearly noticed that $[\text{KTP}]$ in the medium remained unchanged in the PS free experiments for T-APS and Fe-APS, whereas UV exposure alone significantly contributed to the

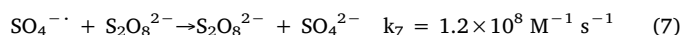
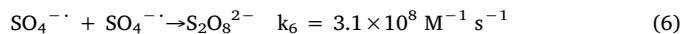
degradation of KTP. This suggests that KTP is thermally and chemically resistant while it is highly sensitive to UV irradiation and undergoes direct photolysis (DP) which was confirmed by the work done by Martinez et al. [47] where KTP was found to be highly susceptible to degradation under UV. On the other hand, inactivated PS had no effect on KTP for a period of 1 h and is expected to remain the same for longer periods (Fig. 3S). This also suggests that PS ($E^\circ = 2.1$ V) is not capable of degrading KTP prior to its activation. However, KTP exhibited high % degradation which reached 92% and 98% after 1 h in T-APS and Fe-APS, respectively, and 100% after only 10 min in UV-APS. It is worth noting that KTP undergoes rapid degradation in UV-APS due to the contribution of DP to KTP removal.

3.1.2. Effect of initial PS concentration in all activated PS systems

The effect of $[PS]_0$ was studied in the three activation methods. The % RSE was calculated only in the case of T-APS where it was possible to easily quantify PS, using the recently developed method in our laboratory by means of a modified HPLC unit [48]. We were not able to trace PS in UV-APS and Fe-APS due to low $[PS]_0$ (e.g. 0.1 mM) and the presence of Fe^{2+} (PS activator) in the sample, respectively. To prevent further degradation of KTP in the presence of Fe^{2+} and PS, the withdrawn sample was quenched with excess MeOH.

3.1.2.1. Thermally activated system. Fig. 3 shows the effect of $[PS]_0$ on % KTP degradation using T-APS. KTP removal was obviously enhanced as $[PS]_0$ increased in the medium; in addition, k_{obs} was positively and linearly correlated to $[PS]_0$ at all studied temperatures which is the same trend observed by several other researchers [36,49,50]. The % RSE ranged between 5.18% and 33.17% at $T = 60^\circ C$, which is about 5 to 10 times higher than the values calculated for both $50^\circ C$ and $40^\circ C$ (0.5–6%). Such observation is mainly due to the fact that KTP becomes more prone to SRs oxidation at higher temperature, which is further supported by the PS consumption values, where PS consumed at each of 40, 50 and $60^\circ C$ experiments at time t (min) of the reaction were very

comparable (Fig. 4S). On the other hand, the maximum % RSE (33.2%) obtained was at $[PS]_0 = 1$ mM and $T = 60^\circ C$ (Fig. 5S), where it decreased significantly as the $[PS]_0$ increased above 1 mM possibly due to the vigorous quenching/parasitic reactions (Eqs. (6) and (7)) [51,52] or the rapid production of high concentration of degradation byproducts [36,44], resulting in the inefficient consumption of PS towards probe removal which was encountered by many research groups [36,42,44].



As for $[PS]_0 < 1$ mM and $T = 60^\circ C$, the % RSE was highest at $[PS]_0 = 0.25$ mM compared to 0.5 and 0.75 mM; however, the % KTP degradation was relatively low (40%) indicating the necessity for longer reaction time. In addition, the observed byproducts were efficiently removed at $[PS]_0 \geq 1$ mM (Fig. 6S). The conditions at which highest % RSE was achieved were later adopted as the optimal conditions in all the other experiments on T-APS.

3.1.2.2. UV activated system. KTP degradation was significantly enhanced by increasing $[PS]_0$ similar to the case of thermal activation. Although KTP degrades rapidly under UV alone, its byproducts remain persistent for longer periods of time (Fig. 7S), which suggests the necessary addition of PS. Fig. 4 demonstrates the positive correlation between k_{obs} and $[PS]_0$. It was enough to spike the solution with only 0.1 mM PS to induce faster degradation of KTP and its byproducts. In fact, KTP reached full degradation after 7 min of reaction time, therefore $[PS]_0 = 0.1$ mM was adopted for all other experiments conducted in UV-APS, especially that this system showed perfect sustainability as explained later in Section 3.6. The % RSE was not quantified due to the decrease of $[PS]_t$ below detectable concentrations (see Text S1, Section 2.2.2).

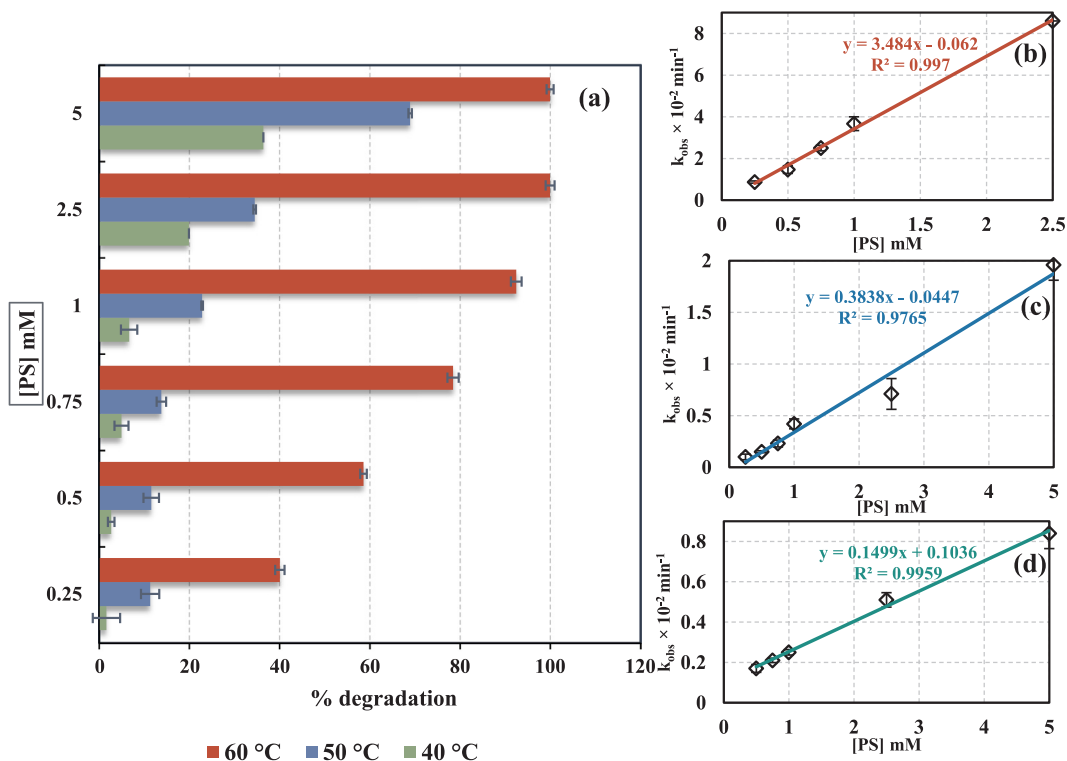


Fig. 3. The evolution of (a) % KTP degradation and (b, c, d) k_{obs} as a function of $[PS]_0$ and temperature in T-APS. Experimental conditions: $[KTP]_0 = 7.87 \mu\text{M}$, $[PS]_0 = 0.25\text{--}5$ mM. $T = 40\text{--}60^\circ C$. Error bars representing standard deviation are calculated at 95% confidence level, and uncertainties on k_{obs} were calculated from standard deviation on the slope of $\ln([KTP]_t/[KTP]_0)$ vs. t (min), determined after using the LINEST function of Microsoft excel. $pH_{i(\text{avg})} = 6.15$, $pH_{f(\text{avg})} = 4.05$.

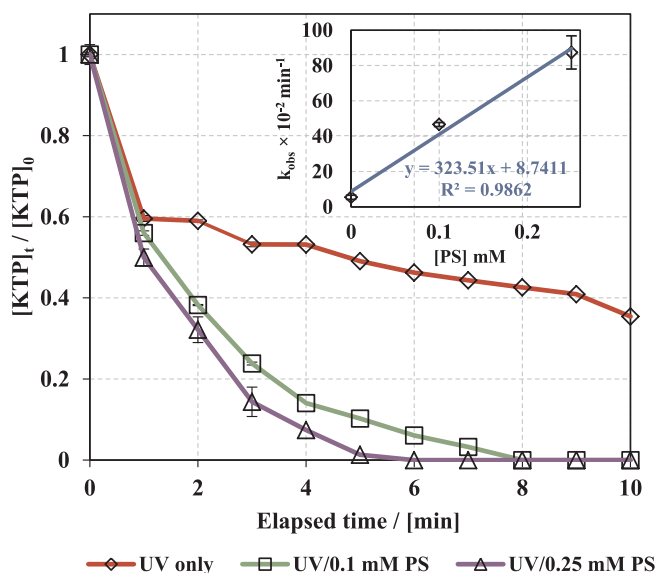
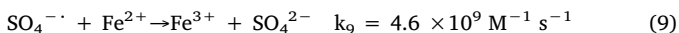
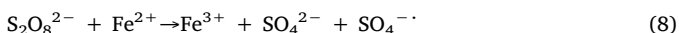


Fig. 4. Effect of $[PS]_0$ on KTP degradation and k_{obs} in UV-APS. Experimental conditions: $[KTP]_0 = 7.87 \mu\text{M}$, $[PS]_0 = 0\text{--}0.25 \text{ mM}$. Error bars representing standard deviation are calculated at 95% confidence level, and uncertainties on k_{obs} are calculated from the standard deviation on the slope of $\text{Ln}([KTP]_t/[KTP]_0)$ vs. t (min), determined after using the LINEST function of Microsoft excel. $\text{pH}_{i(\text{avg})} = 6.15$, $\text{pH}_{f(\text{avg})} = 5.88$.

3.1.2.3. Chemically activated system. The effect of $[PS]_0$ in Fe-APS was highly dependent on its ratio to $[\text{Fe}^{2+}]_0$. To assess this effect, three different $[PS]_0$ (0.1, 0.5 and 1 mM) and $[\text{Fe}^{2+}]_0:[PS]_0$ (1:1, 1:5, 1:10) ratios were tested in an array of nine combinations.



PS gets chemically activated through Eq. (8) while SRs get quenched in excess Fe^{2+} through Eq. (9) [53]. Therefore, the aim of ratio optimization is to minimize as much as possible SRs quenching (9) while maintaining efficient KTP degradation. Fig. 5 shows that the highest % KTP degradation (75% after 1 h) is achieved at the lowest $[PS]_0$ and $[\text{Fe}^{2+}]_0$ used i.e. 0.1 mM at 1:1 M ratio. This result is attributed to the rapid consumption of Fe^{2+} by PS (Eq. (8)), therefore preventing any quenching reaction. However, at higher concentrations, competition between activation and quenching reactions becomes more significant due to the rapid production of SRs in the presence of excess $[\text{Fe}^{2+}]$ with respect to $[PS]$ and the very high reaction rate between SRs and Fe^{2+} . On the other hand, the % KTP degradation increased with the increase in $[PS]_0$ and $[\text{Fe}^{2+}]_0$ when the ratio was 1:10, indicating that the quenching reaction is less likely to occur at such ratio due to the full consumption of Fe^{2+} by PS in solution; therefore, the % degradation was directly correlated to $[PS]_0$ initially present in the medium. At 1:5 $[\text{Fe}^{2+}]_0:[PS]_0$ ratio, all $[PS]_0$ resulted in fair % degradation ($\geq 55\%$), where the highest % degradation (98%) was achieved when $[PS]_0 = 0.5 \text{ mM}$ and $[\text{Fe}^{2+}]_0 = 0.1 \text{ mM}$ due to the nearly full transformation of Fe^{2+} into Fe^{3+} (Eq. (8)). The % degradation was lower elsewhere either due to the quenching effect when $[\text{Fe}^{2+}]_0$ is high ($[\text{Fe}^{2+}]_0 = 0.2 \text{ mM}$ and $[PS]_0 = 1 \text{ mM}$), or the insufficient $[\text{Fe}^{2+}]_0$ able to activate all the PS for enhanced degradation ($[\text{Fe}^{2+}]_0 = 0.02 \text{ mM}$ and $[PS]_0 = 0.1 \text{ mM}$). This was further supported by the poor by-product removal (Fig. 8S) in almost all cases where more than 60% of the byproduct remained persistent, except for 0.1:1 and 0.1:0.5 mM $[\text{Fe}^{2+}]_0:[PS]_0$ where the % byproduct remaining was found to be 37% and 27%, respectively. Therefore, $[\text{Fe}^{2+}]_0:[PS]_0$ ratio optimization is essential to overcome both the insufficient probe degradation and quenching of SRs by Fe^{2+} [37]. The initial conditions $[PS]_0 = 0.5 \text{ mM}$

and $[\text{Fe}^{2+}]_0 = 0.1 \text{ mM}$ were adopted for later experiments.

3.2. Temperature effect in thermally activated system

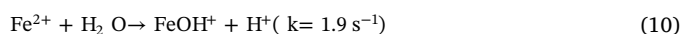
Fig. 6 shows the effect of temperature on the oxidative degradation of KTP in T-APS. The pseudo first order reaction models presented in Fig. 6a show a clear dependence on temperature (R^2 obtained from the plot of $\text{Ln}([KTP]_t/[KTP]_0) > 0.95$, Table 1). Specifically, the % KTP removal was improved from 5% at 40 °C to 100% at 70 °C after a period of 1 h. This observation is in accordance with previous work done by Ghanch et al. on T-APS [38,40,54]. This is mainly attributed to the increase in the concentration of SRs in the reaction medium, and the consequent increase in the pseudo first order reaction rates constants ($k_{obs} \text{ min}^{-1}$, Table 1) as the temperature is increased. This leads to a higher vulnerability of KTP towards radical-based oxidation [55–57]. The half-lives of KTP calculated from the pseudo first order equation ($t_{1/2} = \text{Ln}2/k_{obs}$) highly increased from 5.12 min at 70 °C to 866 min at 40 °C (Table 1). The stability of pharmaceuticals can be determined from Arrhenius studies and can be used in order to predict the activation energy (E_A) of these compounds by performing forced degradation studies at elevated temperatures [58]. To calculate E_A , reaction rates were obtained at various temperature conditions (40–70 °C) and showed perfect fitting in the Arrhenius equation ($R^2 = 0.9936$, Fig. 6b) designated by the following relation between k_{obs} and temperature:

$$\text{Ln}(k_{obs}) = \text{Ln}A - \frac{E_A}{RT}$$

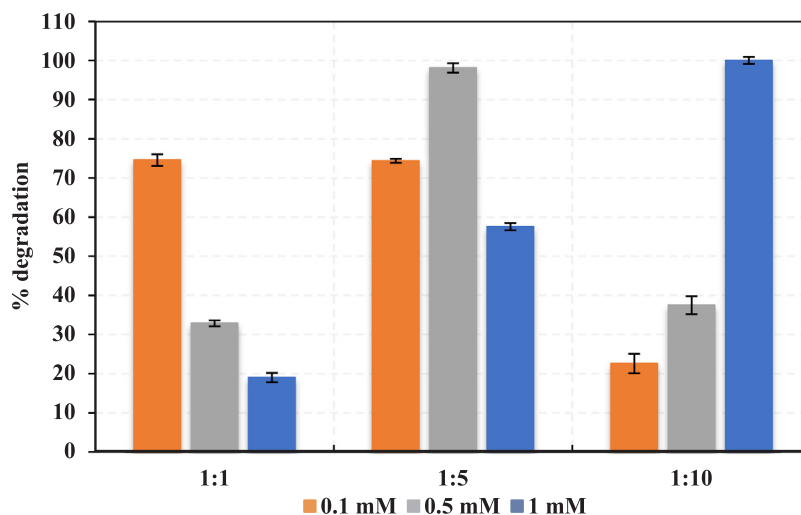
where A is the pre-exponential factor found from the intercept of the Arrhenius plot, E_A is the activation energy (J mol^{-1}), T is the temperature (K) and R the universal gas constant ($R = 8.314 \text{ J mol}^{-1} \text{ K}^{-1}$). Based on the above parameters, E_A was found to be 157.02 (± 8.9) kJ mol^{-1} which is slightly deviated from the E_A obtained by Feng et al. [36] on T-APS applied to KTP systems, which was calculated using the same model and was found to be 169.74 kJ mol^{-1} . The E_A obtained is also comparable to that of other commonly used pharmaceuticals such as ibuprofen (168 kJ mol^{-1}) [38], carbamazepine (168 kJ mol^{-1}) [56], bisoprolol (120 kJ mol^{-1}), triclosan (121 kJ mol^{-1}) [59], as well as naproxen (155 kJ mol^{-1}) [40]. This suggests that the T-APS can be used as a successful treatment option for the removal of mixtures of commonly used pharmaceuticals [36].

3.3. pH effect on KTP degradation kinetics in all activated PS systems

KTP degradation was studied under acidic (pH 4), neutral (pH 7) and basic (pH 11) conditions at constant phosphate buffer strength, $[PB] = 10 \text{ mM}$. Fig. 7 shows the obtained k_{obs} (min^{-1}) values of KTP degradation as a function of time for buffer free and buffer-controlled conditions in T-APS, Fe-APS, and UV-APS. Results clearly show that pH has detrimental effects on KTP degradation in Fe-APS, where k_{obs} dropped significantly from $4.68 \times 10^{-2} \text{ min}^{-1}$ in buffer free medium to $0.65 \times 10^{-2} \text{ min}^{-1}$ at pH 4 and $0.17 \times 10^{-2} \text{ min}^{-1}$ at pH 7. No degradation was observed at pH 11 during the time of study, therefore no k_{obs} value was obtained. These results can be interpreted by the effect of various pH values on the oxidation of ferrous ions to ferric ions. First, Fe^{2+} forms Fe^{2+} complexes when the pH is higher than 4 as indicated by the following equation [60,61]:



At further higher pHs (neutral and basic), $\text{Fe}(\text{OH})_2$ formation is suspected; both $\text{Fe}(\text{OH})_2$ and FeOH^+ have much lower activity towards PS than uncomplexed Fe^{2+} , leading to significantly lower concentration of SRs in the medium. The effect of neutral and basic media on KTP degradation rate was further proved by the cloudiness observed when Fe^{2+} was added to the buffered solutions (pHs 7 and 11) indicating the plausible formation of ferric hydroxide ions such as FeOH_2^+ , $\text{Fe}_2(\text{OH})_2^{4+}$, $\text{Fe}(\text{OH})_2^+$, $\text{Fe}(\text{OH})_3$ and $\text{Fe}(\text{OH})_4^-$ as noted by Rao et al.

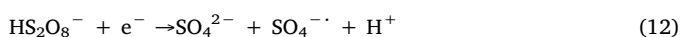


[PS] ₀ (mM)	[Fe ²⁺]:[PS]		
	1:1	1:5	1:10
0.1	0.92 ± 0.13	2.00 ± 0.20	0.35 ± 0.04
0.5	0.41 ± 0.11	4.68 ± 0.30	0.66 ± 0.10
1	0.10 ± 0.01	0.97 ± 0.20	4.77 ± 0.30

Fig. 5. Effect of [PS]₀ and [Fe²⁺]₀ on % KTP degradation and k_{obs} in Fe-APS. Experimental conditions: [KTP]₀ = 7.87 μM, [PS]₀ = 0.1–1 mM, [Fe²⁺]₀ = 0.01–1 mM. The table summarizes $k_{\text{obs}} \times 10^{-2}$ (min⁻¹) values obtained in all [PS]₀ and ratios studied. $\text{pH}_{\text{I}} (\text{avg}) = 6.15$, $\text{pH}_{\text{F}} (\text{avg}) = 3.23$.

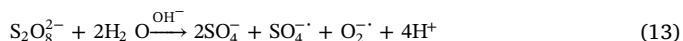
[60]. Aside from the pH effect on the dominant oxidation state of Fe ion in the studied medium, phosphate ions were proven to affect the rate of oxidation of Fe²⁺ to Fe³⁺, the latter having much lower reactivity towards persulfate. Mitra et al. [62] studied the effect of buffer concentration and pH on the oxidation of iron, which showed a positive correlation between the concentration of phosphate buffer and the rate of conversion of Fe²⁺ into Fe³⁺. In addition, this effect was shown to be amplified at higher pHs [62], while iron species can form different complexes with PB (e.g. Fe(H₂O)₄(H₂PO₄)⁺, Fe(H₂O)₄(H₂PO₄)₂, Fe(H₂O)₄(PO₄)₂⁴⁻, etc.) and consequently hindering PS activation [41,63]. Therefore, KTP degradation rate significantly decreased due to the oxidation of Fe²⁺ in the presence of PB and the formation of iron-buffer complexes, and neutral and basic media contributed to the formation of ferric hydroxide ions, which have very low activity towards persulfate activation [60,61].

On the other hand, the effect of pH in both T-APS and UV-APS followed the same expected trend: Acidic (pH 4) media were suitable for KTP degradation enhancement as indicated by the observed reaction rate values obtained, where k_{obs} was improved from $3.6 \times 10^{-2} \text{ min}^{-1}$ to $5.2 \times 10^{-2} \text{ min}^{-1}$ in the case of T-APS, and from $47.1 \times 10^{-2} \text{ min}^{-1}$ to $60.4 \times 10^{-2} \text{ min}^{-1}$ in the case of UV-APS for the unbuffered and pH 4 buffered solutions respectively. This result is in agreement with the previous research done by Feng et al. [36] where observed reaction rates increased from 0.023 min^{-1} in unbuffered media to 0.18 and 0.19 min^{-1} at pHs 3 and 5, respectively. Under acidic pH, PS activation is assisted by acid catalyzed mechanism according to Eqs. (11) and (12) [36]:



However, under alkaline conditions, KTP degradation rates were enhanced in UV-APS while inhibited in T-APS. In general, alkaline media enhance PS activation through the well-known base activation method of PS as reported by several research groups [45,64,65]. PS is

activated under alkaline conditions through the following reaction pathway (Eq. (13)) [37]:



Hydroxyl radicals (HRs) can be generated from SRs as well through the following reaction (Eq. (14)) [66]:



HR (OH[·], E⁰ = 2.7) is known to be very effective in the degradation of a wide range of OCs in water and wastewater [1,67]. Therefore, the occurrence of HRs in addition to SRs enhances the degradation of OCs in the medium. This effect was observed in the case of UV-APS ([PS]₀ = 0.1 mM) in alkaline media (pH = 11), designated by the increase in k_{obs} of KTP degradation from $47.1 \times 10^{-2} \text{ min}^{-1}$ in non-buffered media to $50.2 \times 10^{-2} \text{ min}^{-1}$ in alkaline media. However, an opposite effect was observed in T-APS ([PS]₀ = 1 mM) media, designated by the decrease in k_{obs} from $3.6 \times 10^{-2} \text{ min}^{-1}$ in non-buffered media to $2.4 \times 10^{-2} \text{ min}^{-1}$ in alkaline media. Unlike the case of UV-APS, the following parasitic/radical quenching reaction (Eq. (15)) might have been taking place due to the higher [PS]₀ used (10 times that used in UV-APS), which lead to the increase in the density of SRs and HRs in the medium and consequently the decrease in the rate of KTP degradation [66].



Finally, KTP degradation was slightly inhibited in neutral media, designated by the decrease in k_{obs} values from $3.6 \times 10^{-2} \text{ min}^{-1}$ to $1.91 \times 10^{-2} \text{ min}^{-1}$ in T-APS, and from $4.71 \times 10^{-1} \text{ min}^{-1}$ to $3.95 \times 10^{-1} \text{ min}^{-1}$ in UV-APS. As it can be noticed from the Table of pHs (Fig. 7), pH values in non-buffered media are closer to acidic conditions (where enhancement in k_{obs} values was noticed) than neutral conditions, which explains the decrease in reaction rates in neutral media compared to non-buffered media.

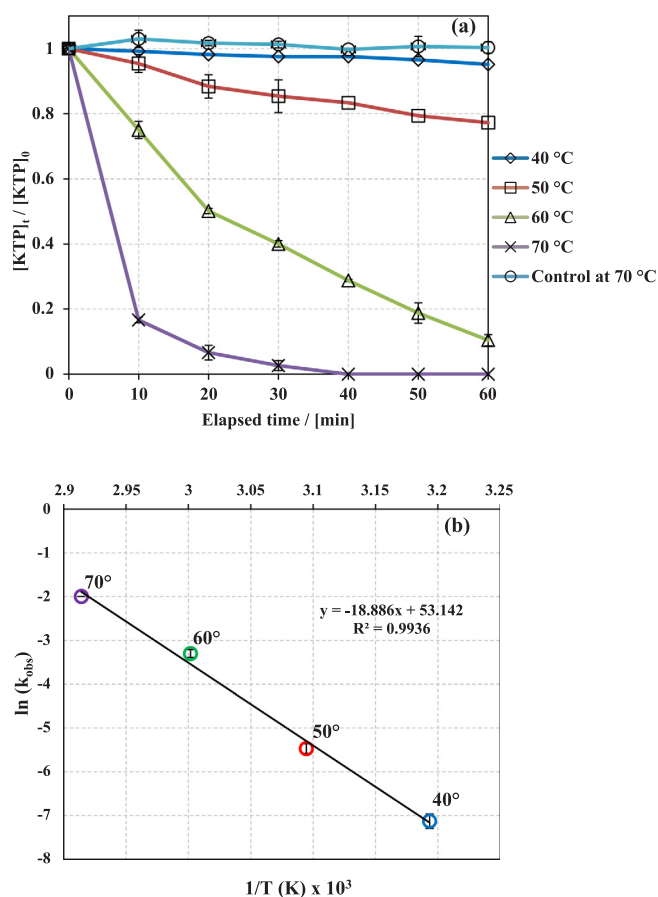


Fig. 6. (a) Temperature effect on the degradation of KTP via T-APS. Experimental conditions: $[KTP]_0 = 7.87 \mu\text{M}$, $[PS]_0 = 1.0 \text{ mM}$. The control experiment was done at 70°C in PS-free solution. Error bars representing standard deviation are calculated at 95% confidence level. (b) Arrhenius plot for the temperature effect experiments. Uncertainties were calculated from standard deviation on the slope determined after using the LINEST function of Microsoft excel. pH_i and pH_f values are reported in Table 1.

Table 1

k_{obs} calculated at different temperatures in T-APS.

Temperature ($^\circ\text{C}$)	$k_{\text{obs}} \times 10^{-2} (\text{min}^{-1})$	R^2	$t_{1/2} (\text{min})$	pH_i	pH_f
40	0.08 ± 0.01	0.9515	866 ± 110	6.12	5.63
50	0.42 ± 0.05	0.9748	165 ± 20	5.90	5.20
60	3.70 ± 0.30	0.9840	19 ± 2	6.30	4.62
70	13.55 ± 0.01	1.0000	5.12 ± 0.01	5.83	4.00

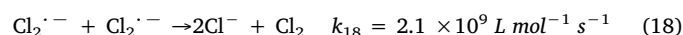
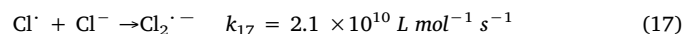
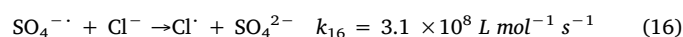
¹ Experimental conditions: $[KTP]_0 = 7.87 \mu\text{M}$, $[PS]_0 = 1 \text{ mM}$. Uncertainties on k_{obs} were calculated from standard deviation on the slope of $\ln([KTP]_t/[KTP]_0)$ vs. t (min), determined after using the LINEST function of Microsoft excel.

3.4. Matrix effect in all activated PS systems

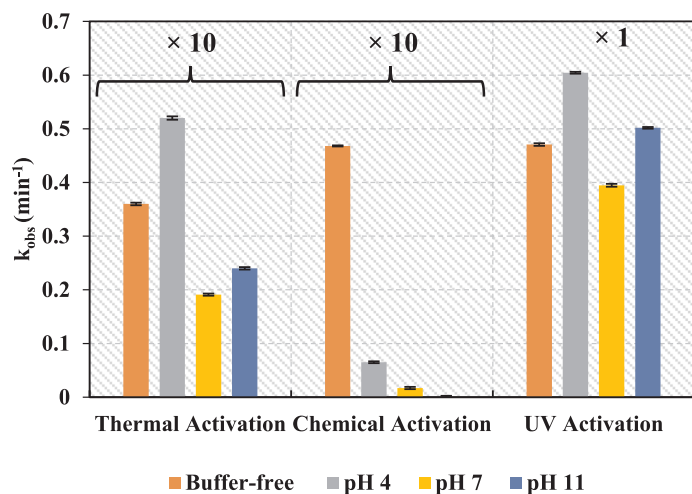
3.4.1. Case of chlorides

The effect of common anions in natural water samples was tested on KTP degradation in T-APS, Fe-APS, and UV-APS. In order to mimic natural water conditions, three different concentrations of chloride ions [68,69] corresponding to fresh water ($[\text{NaCl}] = 2,00 \text{ mg L}^{-1}$), brackish water ($[\text{NaCl}] = 2,000 \text{ mg L}^{-1}$), and saline water ($[\text{NaCl}] = 20,000 \text{ mg L}^{-1}$) were examined. Fig. 8 shows the % degradation and k_{obs} values under the aforementioned conditions. It can be clearly noticed that Fig. 8a and b show a similar trend of variation in % degradation and k_{obs} in salinity experiments in T-APS and UV-APS. In

particular, fresh water matrices enhanced % KTP degradation from 92% (Cl^- free) to 100%, accompanied by a noticeable increase in k_{obs} from $3.6 \times 10^{-2} \text{ min}^{-1}$ (Cl^- free) to $13.8 \times 10^{-2} \text{ min}^{-1}$ in T-APS. However, in the brackish water experiment, % degradation and k_{obs} values were comparable to that of chloride free medium, with a very slight decrease in the % degradation i.e. 88% and nearly same $k_{\text{obs}} = 3.1 \times 10^{-2} \text{ min}^{-1}$. Nevertheless, increasing the $[\text{NaCl}]$ to $20,000 \text{ mg L}^{-1}$ had a significant inhibition effect on KTP degradation which was characterized by the drop in the % degradation to 42% and k_{obs} to $0.79 \times 10^{-2} \text{ min}^{-1}$. Similarly, the % KTP degradation in UV-APS was not affected in fresh water matrix, while k_{obs} increased slightly from $47.1 \times 10^{-2} \text{ min}^{-1}$ (Cl^- free) to $50.45 \times 10^{-2} \text{ min}^{-1}$ (fresh water). In the brackish and saline matrices, the % KTP degradation and k_{obs} values decreased to reach 97% and $31.86 \times 10^{-2} \text{ min}^{-1}$ and 93% and $25.19 \times 10^{-2} \text{ min}^{-1}$, respectively (Fig. 8b). These results are in accordance with previous research done on UV/PS based chloramphenicol removal by Ghauch et al. [44] and Tan et al. [70] where $[\text{Cl}^-]$ ranging between 1 and 10 mM (58.4 and 584 mg L^{-1} of NaCl) enhanced the degradation of the contaminant in PS activated systems. This improvement in degradation is attributed to the oxidative power enhancement of the reactive medium due to the generation of chloride radicals (Cl^\cdot) (Eq. (16)), which react with chloride ions (Eq. (17)) to form the reactive chlorine radicals $\text{Cl}_2^{\cdot-}$ ($E^0 = 2.09 \text{ V}$). However, the observed inhibition in KTP degradation in brackish and more significantly in saline media, can be assigned to the chlorine radical-radical quenching effect (Eq. (18)), particularly in brackish (2000 mg L^{-1}) and saline ($20,000 \text{ mg L}^{-1}$) matrices where $[\text{Cl}^-]$ is above 10 mM (584 mg L^{-1} of NaCl) since the concentrations of $[\text{Cl}^\cdot]$ and $[\text{Cl}_2^{\cdot-}]$ become more significant (Eq. 1618). Comparable results were also established by Bennedsen [71] and Deng [72] where the degradation efficiency was obviously inhibited when $[\text{Cl}^-]_0$ was above 28 mM (1635 mg L^{-1} of NaCl) in T-APS ($[PS]_0 = 5 \text{ mM}$, $T = 65^\circ\text{C}$) and 10 mM (584 mg L^{-1} of NaCl) in UV-APS ($[PS]_0 = 1 \text{ mM}$, $I_0 = 153 \mu\text{W cm}^{-2}$), respectively.



On the other hand, KTP degradation was markedly inhibited in Fe-APS under fresh, brackish, and saline matrices. This was demonstrated by the absence of any noticeable degradation in saline media, and by the respective decrease of % KTP degradation and k_{obs} by 86% and $4.5 \times 10^{-2} \text{ min}^{-1}$ in brackish media and by 25% and $3.2 \times 10^{-2} \text{ min}^{-1}$ in fresh water media. This suggests the direct interference of Cl^- in the activation process of PS, mainly through changing the available species Fe^{2+} ions at various $[\text{Cl}^-]$. The major ferrous chloride complexes present at room temperature in aqueous acidic solutions ($\text{pH}_{i,f} = 6.14\text{--}3.19$, Fig. 7), are $\text{Fe}(\text{H}_2\text{O})_6^{2+}$, $\text{Fe}(\text{H}_2\text{O})_5\text{Cl}^+$, and $\text{Fe}(\text{H}_2\text{O})_4\text{Cl}_2$ [73]. It was found that as the $[\text{Cl}^-]$ increases in the solution, the iron speciation shifts from $\text{Fe}(\text{H}_2\text{O})_6^{2+}$ to $\text{Fe}(\text{H}_2\text{O})_5\text{Cl}^+$ and $\text{Fe}(\text{H}_2\text{O})_4\text{Cl}_2$, whose activity towards PS oxidation was never reported in the literature. In addition, the formation of inactive iron complexes was further supported by the observation of an orange suspended matter in the solution just after the addition of Fe^{2+} to the reaction mixture containing previously the corresponding $[\text{Cl}^-]$ to each experiment. The observed inhibition in the degradation extent is consequently attributed to the presence of chloride ions in solution, which becomes more significant with the increase in $[\text{NaCl}]$ from 200 to $20,000 \text{ mg L}^{-1}$. Therefore, UV-APS can be used as an efficient AOP for the treatment of KTP in fresh, brackish, and saline matrices due to the comparable efficiency of oxidation in all three media. However, degradation is only enhanced in fresh water media in the case of T-APS, while it is inhibited otherwise. Finally, the use of Fe^{2+} as PS activator for KTP degradation in natural water samples rich in Cl^- was found to



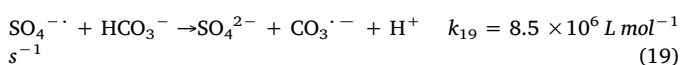
		pHi	pHf
Thermal activation	Non-buffered	6.1	3.85
		4.75	4.05
	Buffered	7.55	7.43
		10.95	10.23
Chemical activation	Non-buffered	6.14	3.19
		3.81	3.59
	Buffered	7.09	7.05
		10.78	10.63
UV activation	Non-buffered	6.21	5.92
		4.13	3.87
	Buffered	7.13	7.10
		11.00	10.83

Fig. 7. k_{obs} obtained from the first order fitting function for T-APS, Fe-APS, and UV-APS at pH values 4, 7, and 11. The table is a summary of pH_i and pH_f for each experiment. Experimental conditions: $[KTP]_0 = 7.87 \mu\text{M}$ and $[PB] = 10 \text{ mM}$ in all systems, $[PS]_0 = 1.0 \text{ mM}$ (T-APS), $[PS]_0 = 0.5 \text{ mM}$ and $[\text{Fe}^{2+}]_0 = 0.1 \text{ mM}$ (Fe-APS), $[PS]_0 = 0.1 \text{ mM}$ (UV-APS). For demonstration purposes, the k_{obs} values for thermal and chemical systems were multiplied by 10.

be inefficient.

3.4.2. Case of bicarbonates

The presence of high concentrations of bicarbonate in the reaction matrix led to significant decrease in the degradation extent and k_{obs} in all three PS activated systems (Fig. 9). k_{obs} decreased by 90% and 94% at $[\text{HCO}_3^-]$ of 50 and 100 mM in T-APS, while $[\text{HCO}_3^-] = 1 \text{ mM}$ inhibited k_{obs} to a much lower extent i.e. 30%. A similar trend was also noticed in UV-APS, designated by a moderate decrease in k_{obs} at $[\text{HCO}_3^-] = 1 \text{ mM}$ by 43%, 71% at $[\text{HCO}_3^-] = 50 \text{ mM}$, and 78% at $[\text{HCO}_3^-] = 100 \text{ mM}$. On the contrary, k_{obs} value was not affected in Fe-APS when 1 mM of HCO_3^- was added; however, higher $[\text{HCO}_3^-] = 50$ and 100 mM fully inhibited degradation. The inhibitory effect of HCO_3^- can be explained by the reaction of SRs with HCO_3^- (Eq. (19)) yielding CO_3^{2-} which has moderate oxidative properties ($E^0 = 1.50 \text{ V}$) compared to that of SRs toward KTP.



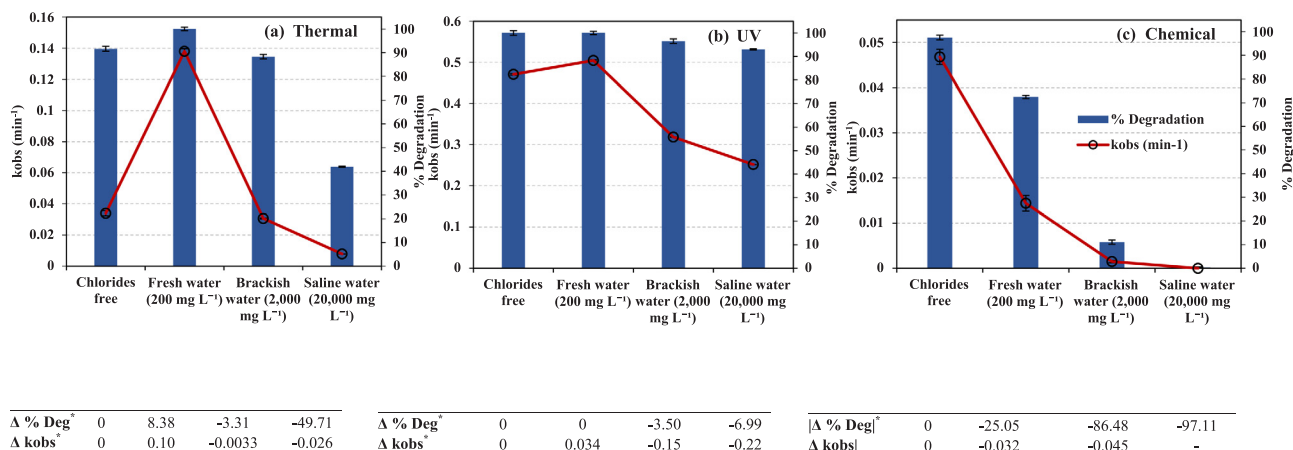
In addition, HCO_3^- reacts with Fe^{2+} to form insoluble complex

(FeCO_3) (Eq. (20)) [74] preventing thereby Fe^{2+} from activating PS.



3.4.3. Case of HA

The effect of humic acids (HA) on the degradation efficiency of the three activation methods has been studied due to their significant abundance in natural waters. The $[\text{HA}]$ ranges typically between 0.1 and 20 mg L^{-1} [75], therefore, three $[\text{HA}]_0$ were adopted: 0.5, 5, and 20 mg L^{-1} . Fig. 10 shows the effect of various $[\text{HA}]$ on KTP degradation and on k_{obs} in T-APS, UV-APS, and Fe-APS. As it can be noticed, HA inhibited KTP degradation in T-APS where k_{obs} decreased from $3.6 \times 10^{-2} \text{ min}^{-1}$ in HA free experiment to 1.82, 1.28 and $0.73 \times 10^{-2} \text{ min}^{-1}$ as the $[\text{HA}]$ increased from 0.5 to 20 mg L^{-1} (Fig. 10a). This observation is in accordance with the work done by Feng et al. [36] where k_{obs} of KTP degradation decreased from 0.08 to 0.02 min^{-1} as the $[\text{HA}]$ increased from 0 to 40 mg L^{-1} in T-APS. Similarly, KTP degradation was inhibited in UV-APS, indicated by the decrease in k_{obs} from $47.1 \times 10^{-2} \text{ min}^{-1}$ in HA free solutions to 23.04 and $7.03 \times 10^{-2} \text{ min}^{-1}$ at $[\text{HA}] = 5$ and 20 mg L^{-1} , respectively;



$$^* \Delta \% \text{ Deg} = \% \text{ Deg}_{\text{chlorides-free}} - \% \text{ Deg}_{\text{fresh/brackish/saline}}$$

$$^* \Delta k_{obs} = k_{obs \text{ chlorides-free}} - k_{obs \text{ fresh/brackish/saline}}$$

Fig. 8. The effect of existing Cl^- (200–20,000 mg L^{-1}) on k_{obs} and %KTP degradation in (a) T-APS, (b) UV-APS, and (c) Fe-APS. Experimental conditions: $[KTP]_0 = 7.87 \mu\text{M}$ in the three systems, $[PS]_0 = 1 \text{ mM}$ and $T = 60 \text{ }^\circ\text{C}$ (T-APS), $[PS]_0 = 0.1 \text{ mM}$ (UV-APS), $[PS]_0 = 0.5 \text{ mM}$ and $[\text{Fe}^{2+}]_0 = 0.1 \text{ mM}$ (Fe-APS). pH_i (avg) = 6.15, pH_f (avg) = 4.23 (T-APS), pH_f (avg) = 5.67 (UV-APS), pH_f (avg) = 3.35 (Fe-APS).

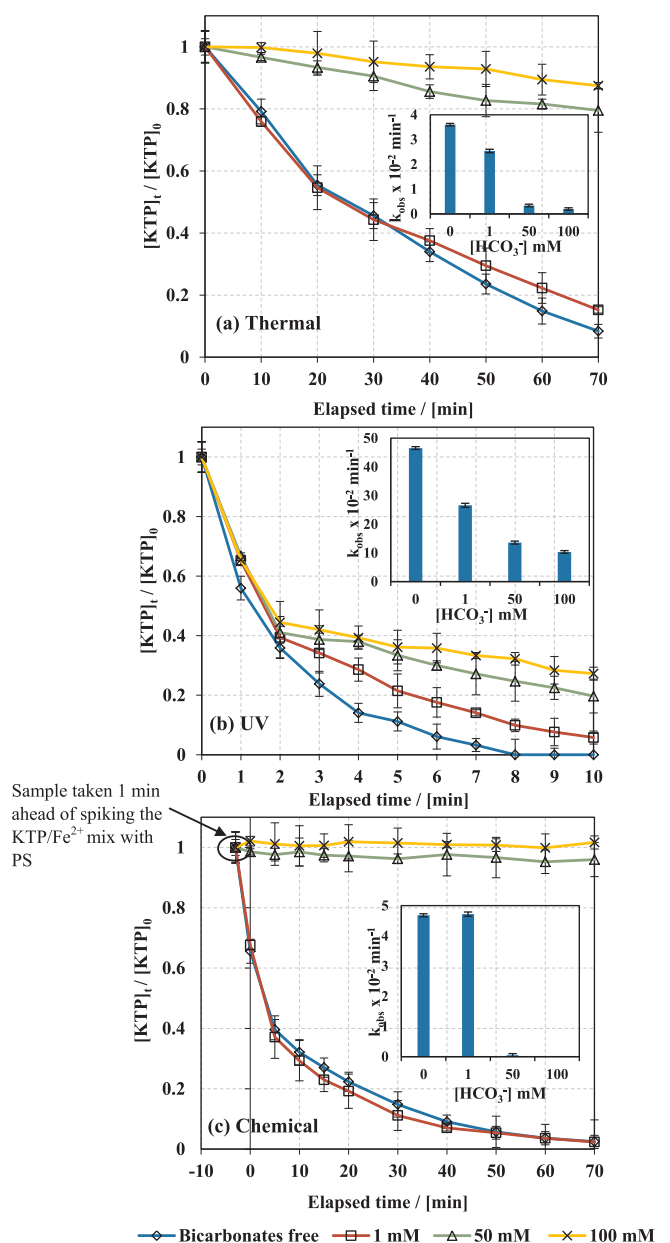
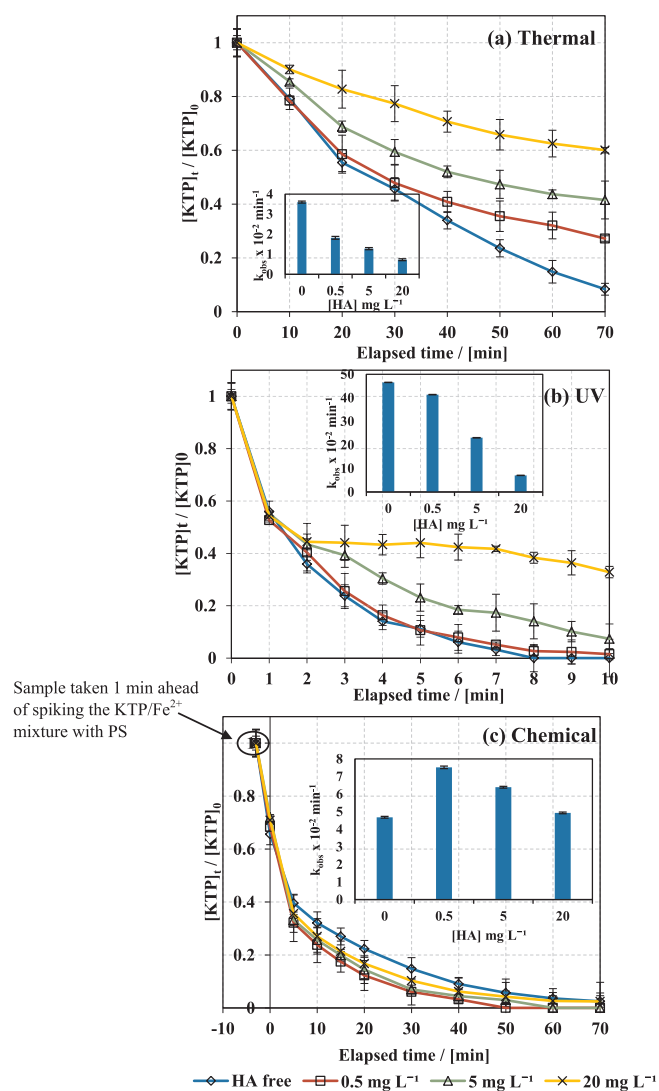


Fig. 9. The effect of existing HCO_3^- (1–100 mM) on KTP degradation in (a) T-APS, (b) UV-APS, and (c) Fe-APS. Experimental conditions: $[KTP]_0 = 7.87 \mu\text{M}$ in all systems, $[PS]_0 = 1 \text{ mM}$ and $T = 60^\circ\text{C}$ (T-APS), $[PS]_0 = 0.1 \text{ mM}$ (UV-APS), $[PS]_0 = 0.5 \text{ mM}$ and $[Fe^{2+}]_0 = 0.1 \text{ mM}$ (Fe-APS). The insets are plots of k_{obs} vs $[HCO_3^-]$. $pH_{i(\text{avg})} = 6.15$, $pH_{f(\text{avg})} = 5.23$ (T-APS), $pH_{f(\text{avg})} = 6.0$ (UV-APS), $pH_{f(\text{avg})} = 4.20$ (Fe-APS).

however, no significant effect was observed at low $[HA]$ (Fig. 10b). Analogous results were also expressed in the studies done on the degradation of chloramphenicol in UV-APS by Ghauch et al. [44], and in T-APS by Nie et al. [49]. This inhibition in both thermal and UV systems is mainly attributed to the HA's quenching effect due to the presence of abundant electron-rich sites thereby attracting electrophilic species such as SRs and HRs [76–79]. In addition, the considerable decrease in k_{obs} at $[HA] = 20 \text{ mg L}^{-1}$ in UV-APS is also attributed to the inner filter effect induced by HA due to its high absorbance at 254 nm [79,80], which prevents full PS irradiation and consequently its activation. On the other hand, HAs showed enhancing properties towards KTP degradation in Fe-APS which is expressed by the higher values of k_{obs} obtained at all $[HA]$ used compared to HA free solutions (Fig. 10c). It has been noticed that k_{obs} increased from $4.68 \times 10^{-2} \text{ min}^{-1}$ in HA



Sample taken 1 min ahead of spiking the KTP/ Fe^{2+} mixture with PS

Fig. 10. The effect of existing HA ($0.5\text{--}20 \text{ mg L}^{-1}$) on KTP degradation in (a) T-APS, (b) UV-APS, and (c) Fe-APS. Experimental conditions: $[KTP]_0 = 7.87 \mu\text{M}$ in all systems, $[PS]_0 = 1 \text{ mM}$ and $T = 60^\circ\text{C}$ (T-APS), $[PS]_0 = 0.1 \text{ mM}$ (UV-APS), $[PS]_0 = 0.5 \text{ mM}$ and $[Fe^{2+}]_0 = 0.1 \text{ mM}$ (Fe-APS). The insets are plots of k_{obs} vs $[HA]$. $pH_{i(\text{avg})} = 6.15$, $pH_{f(\text{avg})} = 3.55$ (T-APS), $pH_{f(\text{avg})} = 5.52$ (UV-APS), $pH_{f(\text{avg})} = 3.07$ (Fe-APS).

free solutions to $7.52 \times 10^{-2} \text{ min}^{-1}$ at $[HA] = 0.5 \text{ mg L}^{-1}$ which decreased again to reach $6.39 \times 10^{-2} \text{ min}^{-1}$ and $4.93 \times 10^{-2} \text{ min}^{-1}$ at 5 and 20 mg L^{-1} HA, respectively. Several research groups have investigated the influence of HA in Fenton and Fenton like systems to prove that HA could have potential positive effect on contaminant degradation [81–84]. Yet, little research has been done on the enhancement of contaminant degradation under HA matrices in Fe-APS. Many studies on Fenton systems reported that this enhancement is mainly due to the reductive ability of HA obtained by electron transfer towards transition metals, Fe^{3+} in this case, which contributes to the regeneration of Fe^{2+} in the solution [85–88]. Therefore, this process known as Fe^{2+} regeneration catalyzes the overall KTP degradation. Finally, KTP degradation enhancement by HA matrix was inversely proportional to $[HA]$ at very high HA load due to the competition of HA and KTP for SRs.

3.4.4. Case of natural water samples: waste water (WW), sea water (SW), and spring water (SpW)

Results of KTP-spiked natural water samples collected from SW in South Lebanon (location $33^\circ54'11.1''\text{N}$ $35^\circ28'44.8''\text{E}$), from untreated

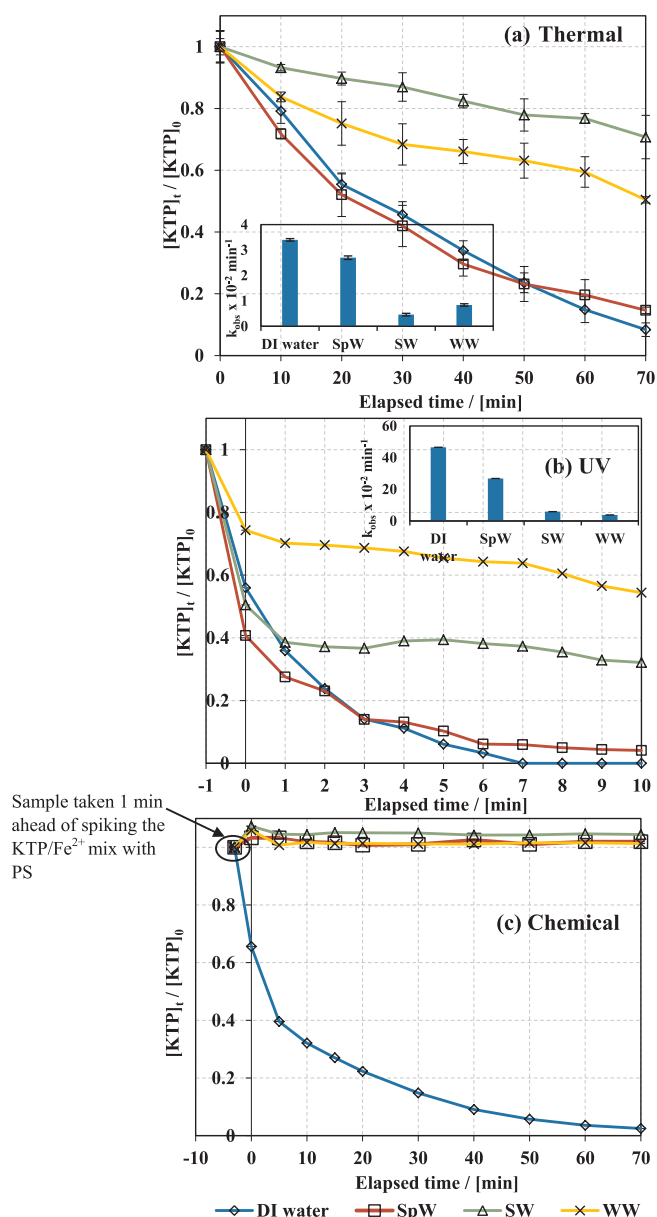


Fig. 11. The effect of natural water samples WW, SW and SpW on KTP degradation in (a) T-APS, (b) UV-APS, and (c) Fe-APS. Experimental conditions: $[KTP]_0 = 7.87 \mu\text{M}$ in all systems, $[PS]_0 = 1 \text{ mM}$ and $T = 60^\circ\text{C}$ (T-APS), $[PS]_0 = 0.1 \text{ mM}$ (UV-APS), $[PS]_0 = 0.5 \text{ mM}$ and $[Fe^{2+}]_0 = 0.1 \text{ mM}$ (Fe-APS). The insets are plots of k_{obs} obtained in the natural water samples. pH_i and pH_f values are reported in Table 2.

municipal WW sewage line discharging into the Mediterranean Sea (location $33^\circ54'08.2''\text{N}$ $35^\circ29'05.0''\text{E}$), and from SpW ($33^\circ44'17.9''\text{N}$ $35^\circ34'12.5''\text{E}$) are presented in Fig. 11. The physical parameters of these samples before and after treatment by each method are presented in Table 2. Experiments applying the three PS activated methods were performed on filtered WW, SW and SpW. Results in the case of T-APS show that the highest drop in k_{obs} was noticed in SW ($0.46 \times 10^{-2} \text{ min}^{-1}$), followed by WW ($0.84 \times 10^{-2} \text{ min}^{-1}$), then SpW ($2.7 \times 10^{-2} \text{ min}^{-1}$). SW contains very high levels of Cl^- (Table 2) which is responsible for quenching SRs in the medium, thereby decreasing % KTP degradation which is in agreement with the results in Section 3.4.1. On the other hand, WW contains a wide range of constituents such as inorganic ions, metals, organic material, etc. that contribute to the high COD as presented in Table 2. In fact, typical WW municipal effluents contain high load of organic material which

competes with KTP for the reaction with SRs, leading to lower degradation extents. KTP degradation was also slightly inhibited in SpW which is attributed to the initial pH value ($\text{pH}_i = 7$), at which degradation is partially inhibited as shown in Section 3.3. On the other hand, k_{obs} decreased significantly in the UV-APS when the experiment was done in SpW ($26.82 \times 10^{-2} \text{ min}^{-1}$), SW ($5.87 \times 10^{-2} \text{ min}^{-1}$) followed by WW ($3.8 \times 10^{-2} \text{ min}^{-1}$). Due to the high turbidity (95 NTU) and TSS (425 mg L^{-1}) in pretreated WW (Table 2), UV irradiation was not reaching the solution efficiently because of light scattering, hence partially preventing PS activation and KTP DP [44,89]. In addition, KTP degradation was inhibited in SW matrix due to the presence of a high Cl^- load which gets involved in PS quenching reactions leading thereby to lower degradation rate. Finally, % degradation and k_{obs} values in the case of SpW was comparable to the case of DI water, where the decrease in both parameters is attributed to the slightly basic pH of the solution which induces inhibitory effect on the degradation process (Section 3.3). All matrices had full inhibitory effect on KTP degradation in Fe-APS. Since pH is a determinant factor in this system, degradation was significantly inhibited due to the basic pH of the studied matrices ($\text{pH} > 7$). On the other hand, high pH values lead to Fe^{2+} precipitation (Section 3.3) which was clearly supported by the increase in TSS values in WW and SW unlike T-APS and UV-APS. Comparing the performance of the three methods in natural water samples, it can be clearly noticed that UV-APS surpasses the T-APS, since it contributes to water disinfection indicated by the decrease of Fecal Coliforms from TNTC to a countable number (58 CFU) in the case of WW (Table 2). The effluent toxicity can be even more reduced in this system if a higher $[PS]_0$ is used as reported in previous studies [90–92].

3.5. Effect of $[PS]_0$ on TOC removal in all activated PS systems

To study the efficiency of the three activation techniques towards mineralization, KTP solutions (10 mg L^{-1}) were treated in the absence of PS (0 mM), under moderate $[PS]_0$ (1 mM) and high $[PS]_0$ (5 mM). $[KTP]_0$ was chosen to be 10 mg L^{-1} ($39.33 \mu\text{M}$) to trace TOC during the reaction time without falling below the detection limit of the TOC analyzer (see SI, Text S1). Fig. 12a shows that KTP is resistant to mineralization at high temperatures (thermal) or in the presence of Fe^{2+} (chemical) at $[PS]_0 = 0 \text{ mM}$, while 11% of TOC was removed after 1 h of treatment under UV irradiation alone. Similar results were observed by Szabo et al. [32] where KTP and its byproducts undergone DP which was expressed by 75% TOC removal after exposure to UV_{254} irradiation. Illes et al. [33] on the other hand, achieved 90% KTP TOC removal in $\text{UV}_{254}/\text{O}_3$ system over a reaction period of 1 h. When $[PS]_0$ 1 mM was used KTP mineralization was enhanced in all three media. Specifically, TOC removal reached 30%, 60%, and 80% in Fe-APS, T-APS and UV-APS respectively (Fig. 12b). This was further heightened at higher $[PS]_0 = 5 \text{ mM}$ where TOC removal reached 48% in Fe-APS, 75% in T-APS, and 95% in UV-APS after 60 min of treatment (Fig. 12c). It is clear that T-APS was more efficient towards mineralization than Fe-APS which is explained by the absence of Fe^{2+} regeneration. This gives advantage to T-APS towards TOC removal in which heat is constantly supplied to the reaction medium. However, UV-APS remains the most efficient method in KTP-TOC removal tests.

3.6. Sustainability tests through successive KTP spiking in all activated PS systems

To assess the sustainability of the activation methods in a long-term oxidation course, the performance of activated PS in the three systems was tested in the scenario of continuous addition of KTP over 60 min time intervals in the case of thermal and chemical systems and for only 10 min in the case of UV-APS. To mimic such scenario, the solution was periodically spiked with 2 mg L^{-1} KTP. Fig. 13 shows KTP degradation results in T-APS, UV-APS, and Fe-APS over five successive spiking cycles, under the initial conditions described in the figure's caption. The

Table 2
Physical properties of waste water, sea water and spring water spiked with KTP before and after treatment in T-APS, UV-APS, and Fe-APS.

Parameters	Units	Waste water					
		Before treatment			After treatment		
					Thermal	UV	Chemical
pH	8.2				8	8	7.9
Fecal Coliforms	⁴ CFU	⁶ TNTC			⁶ TNTC	58	TNTC
Turbidity	⁵ NTU	95			106	95.7	112
¹ TSS	mg L ⁻¹	425			350	315	560
² TDS		4400			4470	4300	4310
sulfates		420			470	420	420
chlorides		3375			2580	2550	4408
³ COD		1106			742	549	260
Parameters	Units	^a Sea water					
		Before treatment			After treatment		
					Thermal	UV	Chemical
pH	8	7.8	7.9		8		
Fecal Coliforms	⁴ CFU	4	2	0	0		
Turbidity	⁵ NTU	1	0.39	0.35	8.08		
¹ TSS	mg L ⁻¹	88	76	83	90		
² TDS		36,600	37,400	34,000	36,600		
sulfates		3500	3600	3800	3500		
chlorides		25,250	25,900	27,500	26,500		
³ COD		970	820	950	720		
Parameters	Units	Spring water					
		Before treatment			After treatment		
					Thermal	UV	Chemical
pH	7	6.7	6.9		6.9		
Fecal Coliforms	⁴ CFU	0	0	0	0		
Turbidity	⁵ NTU	0.63	1.44	0.7	3.96		
¹ TSS	mg L ⁻¹	9	2	5	8		
² TDS		350	436	346	399		
sulfates		16	52	26	34		
chlorides		42.6	25.3	25.6	57		
³ COD		20	22	12	18		

¹ TSS: Total Suspended Solids.

² TDS: Total Dissolved Solids as NaCl.

³ COD: Chemical Oxygen Demand.

⁴ CFU: Colony Forming Unit per 100 mL.

⁵ NTU: Nephelometric Turbidity Unit.

⁶ TNTC: Too Numerous To Count.

* The high COD value observed in sea water is due to the high levels of pollution in the coastal area of Beirut.

first cycle was done as a regular experiment, and then regenerated by spiking the reaction mixture with KTP solution in T-APS and UV-APS and with KTP/Fe²⁺ mix in Fe-APS without altering [PS]₀. The obtained results showed that among the three activation systems, UV-APS was the most sustainable as indicated by the constant % KTP degradation at the end of each cycle (% Deg_{avg} = 93%) (Fig. 13b). This is due to the double effect of DP and activated PS towards the degradation of KTP and its byproducts. On the other hand, T-APS was proven to be less sustainable as indicated by Fig. 13a, where full KTP degradation (100%) was only reached by the end of cycle 1; however, starting from cycle 2, less KTP was degraded (82%), followed by a further decrease to reach 60%, 49% and 41% by the end of cycles 3, 4, and 5, respectively. The Fe-APS was the least sustainable of all, designated by the drop in % KTP degraded from 96% by the end of cycle 1 to 81%, 43%, 30% and 20% by the end of cycles 2, 3, 4 and 5, respectively (Fig. 13c). This is attributed to the change in the ratio of [Fe²⁺] to [PS] which is a main factor as explained in Section 3.1.2.3, and to the accumulation of KTP and its byproducts in the solution. To account for the sustainability for long treatment periods, the % RSE was calculated in the T-APS which

was the only case where PS quantification was possible, as mentioned previously in Section 3.1.2. T-APS had a total PS consumption of 60% after 5 cycles. Regardless of the decrease in % KTP degradation extent, the % RSE increased gradually from 1.55% up to 4.8% from cycle 1 to cycle 5 as shown in the inset of Fig. 13a. This observation is similar to the study done by Ghauch et al. [44] where the % RSE increased although the % degradation of chloramphenicol decreased from cycle 1 to cycle 5 in UV-APS. This proves that both T-APS and UV-APS are sustainable for long term treatment of matrices containing variable [KTP]₀.

3.7. Identification of degradation products and pathways

KTP degradation yielded two common transformation products BP1 and BP2 among the three activation systems, eluted at 5.9 and 6.1 min, respectively (Fig. 14). (+) ESI was adopted since it showed a higher sensitivity compared to (-) ESI. MS analyses were performed under experimental conditions defined in the caption of Fig. 14; KTP is eluted at Rt = 6.6 min and showed a mass spectrum base peak at 255.8 m/z

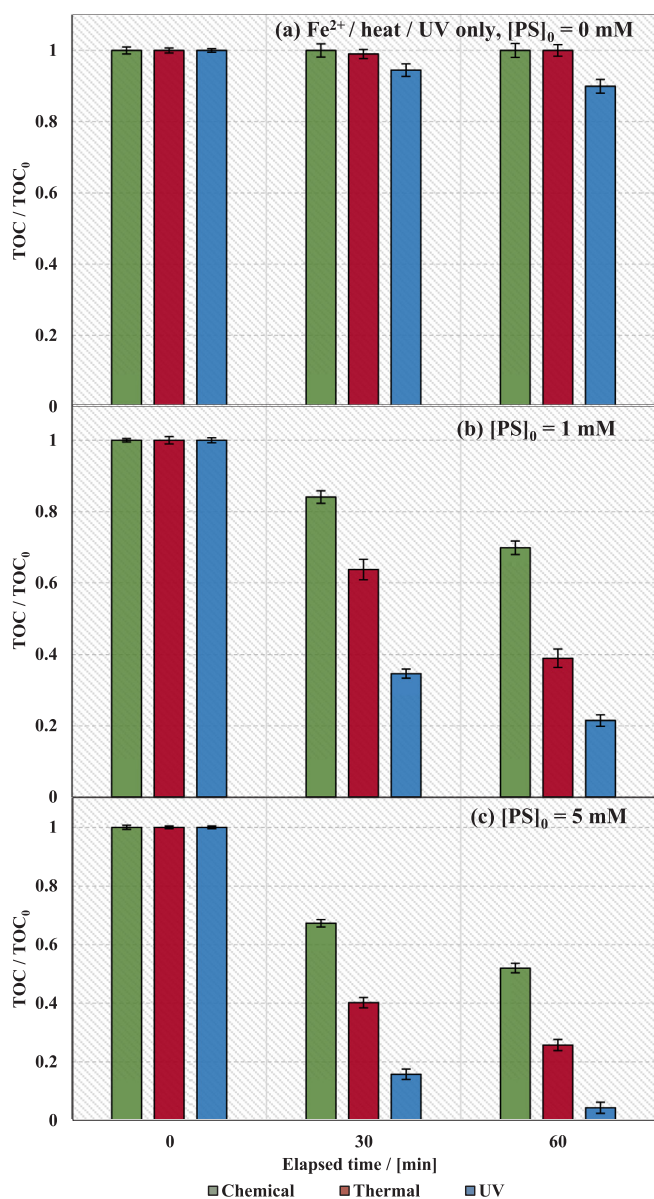


Fig. 12. TOC removal of KTP in T-APS, UV-APS, and Fe-APS (a) in the absence and in the presence of PS at (b) [PS]₀ = 1 mM and (c) [PS]₀ = 5 mM. Experimental conditions: [KTP]₀ = 39.33 μM in all systems. T = 60 °C in T-APS, [Fe²⁺]₀ = ([PS]₀/5) mM in Fe-APS. pH_{i (avg)} = 6.15, pH_{f (avg)} = 4.5 (T-APS), pH_{f (avg)} = 5.35 (UV-APS), pH_{f (avg)} = 3.10 (Fe-APS).

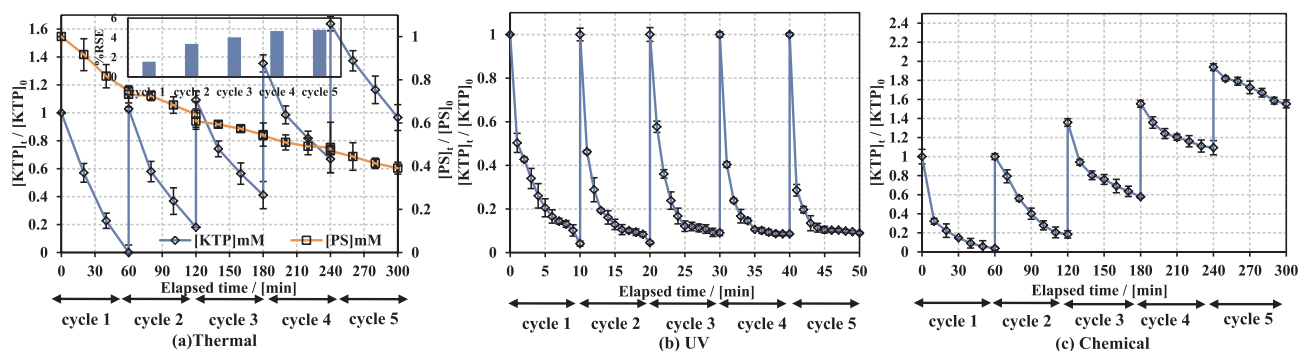


Fig. 13. The effect of successive KTP spiking on the performance of (a) T-APS, (b) UV-APS, and (c) Fe-APS on % KTP degradation and on % RSE in the case of T-APS. Experimental conditions: [KTP]₀ = 7.87 μM/cycle in all systems, [PS]₀ = 2 mM and T = 60 °C (T-APS), [PS]₀ = 0.1 mM (UV), [PS]₀ = 0.5 mM and [Fe²⁺]₀ = 0.1 mM/cycle (Fe-APS). pH_{i (avg)} = 6.15, pH_{f (avg)} = 4.7 (T-APS), pH_{f (avg)} = 5.83 (UV-APS), pH_{f (avg)} = 3.0 (Fe-APS).

corresponding to [M + H]⁺ and additional peaks corresponding to other adduct ions listed in Table 2S. These adducts were mainly Na, K, COOH and FA coupled to KTP in its monomer or dimer form. The latter being also encountered by Ghauch et al. [44] with chloramphenicol molecule analyzed by (+) and (−) ESI. On the other hand, BP1 and BP2 showed two mass spectra base peaks at 229.5 and 245.1 m/z respectively (Tables 3S, 4S). In addition to the listed adducts, MeOH and H₂SO₃ adducts were observed in the mass spectrum of BP1 (Table 4S). A few other MS fragments were also observed but unfortunately not identified.

The general degradation mechanism to form BP1 and BP2 was mainly initiated by decarboxylation [93,94], followed by rearrangement and hydroxylation as shown in Fig. 15. Degradation of KTP to form BP1 and BP2 can be driven either by hydrogen abstraction through HRs or electron abstraction through SRs. HRs in the medium are generated by direct water photolysis in the case of UV [44], or by the reaction of SRs with water which is likely to take place in all investigated systems. However, this pathway, driven by HRs is less probable in chemical system due to the relatively low pH value of the reaction medium. Upon hydrogen or electron abstraction, reactive radical intermediates are generated (Fig. 15) which undergo hydroxylation with water [36] or oxygenation resulting from another SR attack [42]. Transformation products are further subjected to degradation by the available radicals in the medium to achieve partial to full mineralization.

3.8. Economic feasibility study

The economic efficiency was assessed through cost calculation using electrical energy per order (EEO) for T-APS, UV-APS and Fe-APS. EEO is defined as the electric energy in Kilowatt hours (kWh) needed to degrade one order of magnitude of the contaminant per unit volume (m^{−3}), expressed as per Eq. (21) [95]:

$$EEO = \frac{P \times t \times 1000}{V \times \log(C_i/C_f)} \quad (21)$$

Where P (kW) is the power supplied to the system (see text S3), V (L) is the volume treated in time t (h), C_i and C_f are the initial and final concentrations of the contaminant, respectively. Eq. (21) can be simply written as follows:

$$EEO = \frac{38.4 \times P}{V \times k_{obs}} \quad (22)$$

Where k_{obs} (min^{−1}) is the observed reaction rate obtained from the first order fitting functions. The electrical and total system costs were later obtained according to Eqs. (23), (24) [96]:

$$\text{Electrical energy cost ("$/m}^3\text{)} = EEO(\text{kWh/m}^3\text{)} \times \text{power cost ("$/kWh)} \quad (23)$$

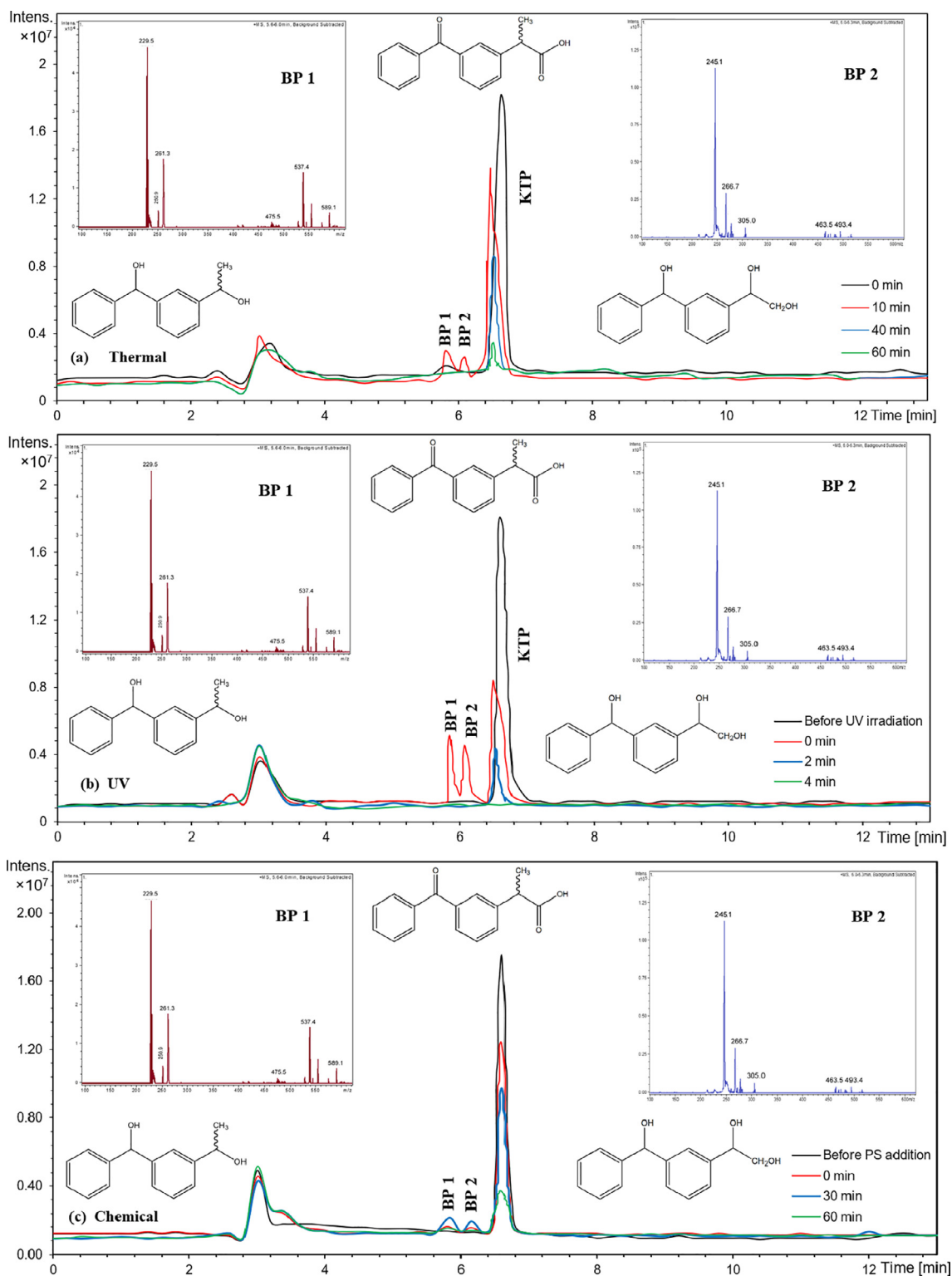


Fig. 14. (+) ESI LC-MS total ion chromatograms of KTP in (a) T-APS, (b) UV-APS, and (c) Fe-APS. The insets in the three figures represent the MS spectra of BP1 and BP2. Experimental conditions: $[KTP]_0 = 39.33 \mu\text{M}$ in all systems. $[PS]_0 = 5 \text{ mM}$, $T = 60^\circ\text{C}$ in T-APS, $[\text{Fe}^{2+}]_0 = 0.5 \text{ mM}$, $[PS]_0 = 2.5 \text{ mM}$ in Fe-APS. $[PS]_0 = 0.5 \text{ mM}$ in UV-APS.

Total system cost ($\$/\text{m}^3$) = electrical energy cost + reagent cost (24)

Table 3 summarizes the total cost of UV, thermal, and chemical activation processes. It is clearly shown that electricity contributes mostly to the total cost in both T-APS and UV-APS, whereas it is assumed to be negligible in Fe-APS. UV-APS was found to be the least costly among the tested methods, followed by Fe-APS and finally T-APS.

However, Fe-APS was found to be inefficient in most of the matrices studied which imposes a great limitation to its use in real life applications. On the other hand, T-APS is considered economically inefficient due to the high electricity (Table 3) and reagent (Table 5S) costs relative to UV-APS. Therefore, UV-APS is found to be the most feasible, robust, effective and efficient when applied in real life environment. In

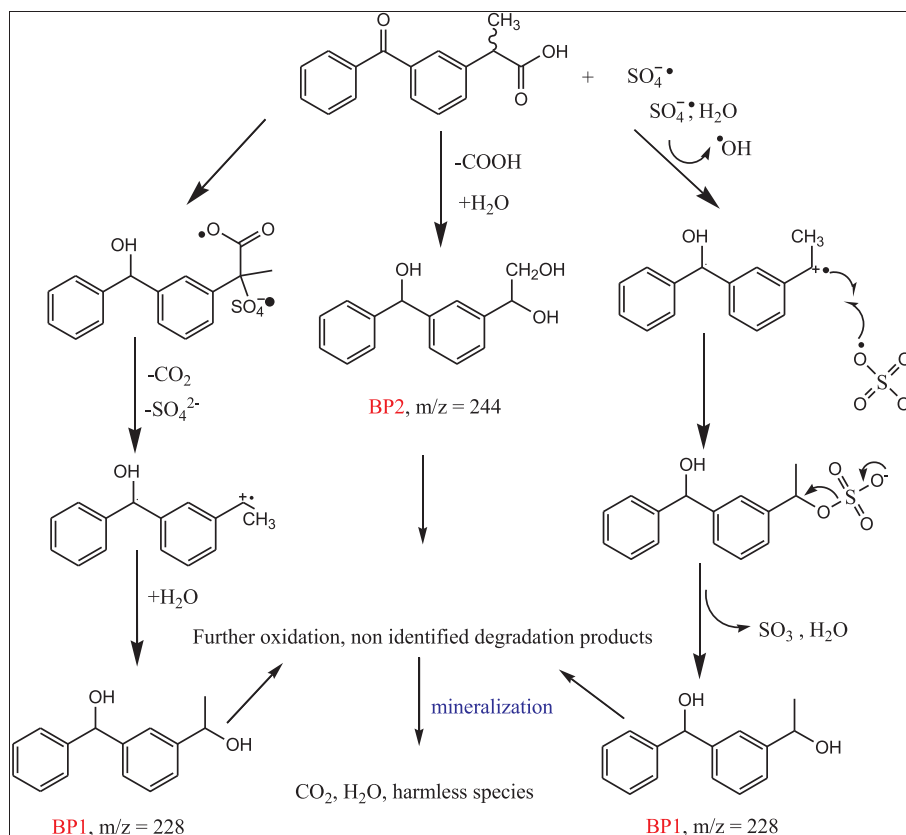


Fig. 15. Proposed degradation mechanism of KTP in T-APS, UV-APS, and Fe-APS. Experimental conditions are similar to those listed in Fig. 14.

Table 3

Economic comparison of the different PS activated systems (UV-APS, T-APS and Fe-APS) obtained at control experimental conditions (Section 3.1): $[KTP]_0 = 7.87 \mu\text{M}$ in all systems, $[PS]_0 = 1 \text{ mM}$ and $T = 60^\circ\text{C}$ (T-APS), $[PS]_0 = 0.1 \text{ mM}$ (UV-APS), $[PS]_0 = 0.5 \text{ mM}$ and $[Fe^{2+}]_0 = 0.1 \text{ mM}$ (Fe-APS).

	UV	Thermal	Chemical
$k_{\text{obs}} \times 10^{-2} (\text{min}^{-1})$	47.100	3.600	4.680
P (kW) ^a	0.011	0.122	–
EEO (kWh/m ³ /order)	2.240	650.600	–
^a Electricity cost (\$/m ³)	0.152	44.176	–
^b Reagent cost (\$/m ³)	0.024	0.238	0.517
Total cost (\$/m ³)	0.176	44.414	0.517

^a Obtained from the “Electric Power Monthly” report including data for November 2017 in the US. Average price of electricity for industrial sector = \$0.0679 [92].

^b See Table 2S.

case the use of UV is not applicable, T-APS is recommended.

4. Conclusion

KTP degradation was studied in T-APS, UV-APS and Fe-APS. Several experimental parameters were tested to investigate the efficiency of the degradation process in all systems. A comparative study was established to come up with the best PS activation technique. UV was found to be the most efficient and robust amongst the systems under study characterized by the high k_{obs} ($47.16 \times 10^{-2} \text{ min}^{-1}$) which was attributed to the DP-assisted degradation of KTP, followed by chemical and thermal systems (4.68×10^{-2} and $3.6 \times 10^{-2} \text{ min}^{-1}$). Degradation in T-APS was found to be pH dependent unlike UV-APS which was unaffected by pH variation, while $\text{pH} > 4$ inhibited degradation to a high extent. TOC analysis showed that the highest KTP mineralization extent (95%) was achieved in UV systems at $[PS]_0 = 5 \text{ mM}$ and

$[KTP]_0 = 10 \text{ mg L}^{-1}$ in 1 h. The effect of several inorganic and organic species commonly found in natural water samples was tested. HA had an enhancing effect in Fe-APS characterized by the increase in k_{obs} values while it slightly inhibited KTP degradation in UV-APS and significantly inhibited KTP degradation in T-APS and Fe-APS while it showed less inhibition extent in UV-APS. Furthermore, Cl^- had nearly no effect on KTP degradation in UV-APS; low $[\text{NaCl}]$ (200 mg L^{-1}) showed to have enhancing properties in T-APS unlike high $[\text{Cl}^-] > 200 \text{ mg L}^{-1}$, while it inhibited KTP degradation in Fe-APS at all concentrations used. The three studied systems were applied to KTP-spiked WW, SW, and SpW samples and showed that UV-APS was the most efficient in terms of KTP degradation and total coliform reduction. It showed perfect sustainability through continuous KTP spiking experiments in comparison to T-APS and Fe-APS which were less sustainable. HPLC/MS analyses were performed to identify the main transformation products and to establish a degradation mechanism. Finally, an economic feasibility study has shown that UV-APS is the most economically efficient method to be applied in real environment. Investigation toward the development of innovative catalysts for PS activation such as Metal-Organic Frameworks (MOFs) is already initiated in our laboratory to improve AOPs toward more sustainability.

Acknowledgments

This research was funded in part by the LNCSR (Award Number 103250), the K Shair CRSL fund (Award Number 103191), and the University Research Board (Award Number 103186) of the American University of Beirut and USAID-Lebanon through The National Academy of Sciences under PEER project 5-18 (Award number 103262). The author is thankful to Joan Younes, Chady Assaf and Samer Khalil for their technical assistance, the personnel of the K. Shair CRSL for their help and Prof. David Sedlak from UC-Berkeley for his

permanent support and valuable remarks on persulfate technology.

Appendix A. Supplementary data

Supplementary data associated with this article can be found, in the online version, at <http://dx.doi.org/10.1016/j.cej.2018.05.118>.

References

- [1] A. Asghar, A.A.A. Raman, W.M.A.W. Daud, Advanced oxidation processes for in-situ production of hydrogen peroxide/hydroxyl radical for textile wastewater treatment: a review, *J. Clean. Prod.* 87 (2015) 826–838.
- [2] V. Burkina, V. Zlabek, G. Zamaratskaia, Effects of pharmaceuticals present in aquatic environment on Phase I metabolism in fish, *Environ. Toxicol. Pharmacol.* 40 (2015) 430–444, <http://dx.doi.org/10.1016/j.etap.2015.07.016>.
- [3] U. Memmert, A. Peither, R. Burri, K. Weber, T. Schmidt, J.P. Sumpter, A. Hartmann, Diclofenac: New data on chronic toxicity and bioconcentration in fish, *Environ. Toxicol. Chem.* 32 (2013) 442–452, <http://dx.doi.org/10.1002/etc.2085>.
- [4] C.G. Daughton, T.A. Ternes, Pharmaceuticals and personal care products in the environment: agents of subtle change? *Environ. Health Perspect.* 107 (1999) 907–938 <http://www.ncbi.nlm.nih.gov/pmc/articles/PMC1566206/>.
- [5] T. Heberer, Occurrence, fate, and removal of pharmaceutical residues in the aquatic environment: a review of recent research data, *Toxicol. Lett.* 131 (2002) 5–17, [http://dx.doi.org/10.1016/S0378-4274\(02\)00041-3](http://dx.doi.org/10.1016/S0378-4274(02)00041-3).
- [6] S. Mompelat, B. Le Bot, O. Thomas, Occurrence and fate of pharmaceutical products and by-products, from resource to drinking water, *Environ. Int.* 35 (2009) 803–814, <http://dx.doi.org/10.1016/j.envint.2008.10.008>.
- [7] T. Kosjek, E. Heath, B. Kompore, Removal of pharmaceutical residues in a pilot wastewater treatment plant, *Anal. Bioanal. Chem.* 387 (2007) 1379–1387, <http://dx.doi.org/10.1007/s00216-006-0969-1>.
- [8] D. Sirbu, D. Curseu, M. Popa, A. Achimas-Cadariu, Z. Moldovan, Environmental risks of pharmaceuticals and personal care products in water, in: n.d.
- [9] T. Heberer, Tracking persistent pharmaceutical residues from municipal sewage to drinking water, *J. Hydrol.* 266 (2002) 175–189.
- [10] C. Zwiener, F.H. Frimmel, Oxidative treatment of pharmaceuticals in water, *Water Res.* 34 (2000) 1881–1885.
- [11] E. Larsson, S. Al-Hamimi, J.Å. Jönsson, Behaviour of nonsteroidal anti-inflammatory drugs and eight of their metabolites during wastewater treatment studied by hollow fibre liquid phase microextraction and liquid chromatography mass spectrometry, *Sci. Total Environ.* 485–486 (2014) 300–308, <http://dx.doi.org/10.1016/j.scitotenv.2014.03.055>.
- [12] S. Zorita, L. Mårtensson, L. Mathiasson, Occurrence and removal of pharmaceuticals in a municipal sewage treatment system in the south of Sweden, *Sci. Total Environ.* 407 (2009) 2760–2770, <http://dx.doi.org/10.1016/j.scitotenv.2008.12.030>.
- [13] A. Tauxe-Wuersch, L.F. De Alencastro, D. Grandjean, J. Tarradellas, Occurrence of several acidic drugs in sewage treatment plants in Switzerland and risk assessment, *Water Res.* 39 (2005) 1761–1772, <http://dx.doi.org/10.1016/j.watres.2005.03.003>.
- [14] J. Rivera-Utrilla, M. Sánchez-Polo, M.Á. Ferro-García, G. Prados-Joya, R. Ocampo-Pérez, Pharmaceuticals as emerging contaminants and their removal from water. A review, *Chemosphere* 93 (2013) 1268–1287, <http://dx.doi.org/10.1016/j.chemosphere.2013.07.059>.
- [15] H.T. Buxton, D.W. Kolpin, Pharmaceuticals, hormones, and other organic wastewater contaminants in US streams, Wiley Online Library, 2005.
- [16] W.H. Organization, Pharmaceuticals in drinking-water, 2011. <http://www.who.int/iris/handle/10665/44630>.
- [17] M. Gros, M. Petrović, D. Barceló, Development of a multi-residue analytical methodology based on liquid chromatography–tandem mass spectrometry (LC–MS/MS) for screening and trace level determination of pharmaceuticals in surface and wastewaters, *Talanta* 70 (2006) 678–690, <http://dx.doi.org/10.1016/j.talanta.2006.05.024>.
- [18] S.K. Behera, H.W. Kim, J.-E. Oh, H.-S. Park, Occurrence and removal of antibiotics, hormones and several other pharmaceuticals in wastewater treatment plants of the largest industrial city of Korea, *Sci. Total Environ.* 409 (2011) 4351–4360, <http://dx.doi.org/10.1016/j.scitotenv.2011.07.015>.
- [19] Y. Luo, W. Guo, H.H. Ngo, L.D. Nghiem, F.I. Hai, J. Zhang, S. Liang, X.C. Wang, A review on the occurrence of micropollutants in the aquatic environment and their fate and removal during wastewater treatment, *Sci. Total Environ.* 473–474 (2014) 619–641, <http://dx.doi.org/10.1016/j.scitotenv.2013.12.065>.
- [20] R. Salgado, R. Marques, J.P. Noronha, G. Carvalho, A. Oehmen, M.A.M. Reis, Assessing the removal of pharmaceuticals and personal care products in a full-scale activated sludge plant, *Environ. Sci. Pollut. Res.* 19 (2012) 1818–1827, <http://dx.doi.org/10.1007/s11356-011-0693-z>.
- [21] A. Lolić, P. Pağa, L.H.M.L.M. Santos, S. Ramos, M. Correia, C. Delerue-Matos, Assessment of non-steroidal anti-inflammatory and analgesic pharmaceuticals in seawaters of North of Portugal: Occurrence and environmental risk, *Sci. Total Environ.* 508 (2015) 240–250, <http://dx.doi.org/10.1016/j.scitotenv.2014.11.097>.
- [22] P.C. Lindholm-Lehto, H.S.J. Ahkola, J.S. Knuutinen, S.H. Herve, Occurrence of pharmaceuticals in municipal wastewater, in the recipient water, and sedimented particles of northern Lake Päijänne, *Environ. Sci. Pollut. Res.* 22 (2015) 17209–17223, <http://dx.doi.org/10.1007/s11356-015-4908-6>.
- [23] H. Mano, F. Takeda, T. Kitamura, S. Okamoto, Y. Suzuki, C.-B. Park, N. Yasui, K. Kobayashi, Y. Tanaka, N. Yamashita, M. Minamiyama, Water quality comparison of secondary effluent and reclaimed water to ambient river water of southern Okinawa Island via biological evaluation, *Environ. Monit. Assess.* 189 (2017) 442, <http://dx.doi.org/10.1007/s10661-017-6160-7>.
- [24] C.I. Nannou, C.I. Kosma, T.A. Albanis, Occurrence of pharmaceuticals in surface waters: analytical method development and environmental risk assessment, *Int. J. Environ. Anal. Chem.* 95 (2015) 1242–1262, <http://dx.doi.org/10.1080/03067319.2015.1085520>.
- [25] N. Nakada, T. Tanishima, H. Shinohara, K. Kiri, H. Takada, Pharmaceutical chemicals and endocrine disruptors in municipal wastewater in Tokyo and their removal during activated sludge treatment, *Water Res.* 40 (2006) 3297–3303, <http://dx.doi.org/10.1016/j.watres.2006.06.039>.
- [26] E. Marco-Urrea, M. Pérez-Trujillo, C. Cruz-Morató, G. Caminal, T. Vicent, White-rot fungus-mediated degradation of the analgesic ketoprofen and identification of intermediates by HPLC–DAD–MS and NMR, *Chemosphere* 78 (2010) 474–481, <http://dx.doi.org/10.1016/j.chemosphere.2009.10.009>.
- [27] J. Fan, G. Zhao, H. Zhao, S. Chai, T. Cao, Fabrication and application of mesoporous Sb-doped SnO₂ electrode with high specific surface in electrochemical degradation of ketoprofen, *Electrochim. Acta* 94 (2013) 21–29, <http://dx.doi.org/10.1016/j.electacta.2013.01.129>.
- [28] M. Murugananthan, S.S. Latha, G.B. Raju, S. Yoshihara, Anodic oxidation of ketoprofen—An anti-inflammatory drug using boron doped diamond and platinum electrodes, *J. Hazard. Mater.* 180 (2010) 753–758, <http://dx.doi.org/10.1016/j.jhazmat.2010.05.007>.
- [29] L. Feng, N. Oturan, E.D. van Hullebusch, G. Esposito, M.A. Oturan, Degradation of anti-inflammatory drug ketoprofen by electro-oxidation: comparison of electro-Fenton and anodic oxidation processes, *Environ. Sci. Pollut. Res.* 21 (2014) 8406–8416, <http://dx.doi.org/10.1007/s11356-014-2774-2>.
- [30] A. Nakajima, M. Tahara, Y. Yoshimura, H. Nakazawa, Determination of free radicals generated from light exposed ketoprofen, *J. Photochem. Photobiol. A Chem.* 174 (2005) 89–97, <http://dx.doi.org/10.1016/j.jphotochem.2005.03.015>.
- [31] R. Salgado, V.J. Pereira, G. Carvalho, R. Soeiro, V. Gaffney, C. Almeida, V.V. Cardoso, E. Ferreira, M.J. Benoliel, T.A. Ternes, A. Oehmen, M.A.M. Reis, J.P. Noronha, Photodegradation kinetics and transformation products of ketoprofen, diclofenac and atenolol in pure water and treated wastewater, *J. Hazard. Mater.* 244–245 (2013) 516–527, <http://dx.doi.org/10.1016/j.jhazmat.2012.10.039>.
- [32] R.K. Szabó, C. Megyeri, E. Illés, K. Gajda-Schrantz, P. Mazellier, A. Dombi, Phototransformation of ibuprofen and ketoprofen in aqueous solutions, *Chemosphere* 84 (2011) 1658–1663, <http://dx.doi.org/10.1016/j.chemosphere.2011.05.012>.
- [33] E. Illés, E. Szabó, E. Takács, L. Wojnárovits, A. Dombi, K. Gajda-Schrantz, Ketoprofen removal by O₃ and O₃/UV processes: Kinetics, transformation products and ecotoxicity, *Sci. Total Environ.* 472 (2014) 178–184, <http://dx.doi.org/10.1016/j.scitotenv.2013.10.119>.
- [34] A.H. Hilles, S.S.A. Amr, R.A. Hussein, O.D. El-Sebaie, A.I. Arafa, Performance of combined sodium persulfate/H₂O₂ based advanced oxidation process in stabilized landfill leachate treatment, *J. Environ. Manage.* 166 (2016) 493–498.
- [35] S.S.A. Amr, H.A. Aziz, M.N. Adlan, Optimization of stabilized leachate treatment using ozone/persulfate in the advanced oxidation process, *Waste Manag.* 33 (2013) 1434–1441.
- [36] Y. Feng, Q. Song, W. Lv, G. Liu, Degradation of ketoprofen by sulfate radical-based advanced oxidation processes: Kinetics, mechanisms, and effects of natural water matrices, *Chemosphere* 189 (2017) 643–651, <http://dx.doi.org/10.1016/j.chemosphere.2017.09.109>.
- [37] L.W. Matzek, K.E. Carter, Activated persulfate for organic chemical degradation: a review, *Chemosphere* 151 (2016) 178–188, <http://dx.doi.org/10.1016/j.chemosphere.2016.02.055>.
- [38] A. Ghauch, A.M. Tuqan, N. Kibbi, Ibuprofen removal by heated persulfate in aqueous solution: a kinetics study, *Chem. Eng. J.* 197 (2012) 483–492, <http://dx.doi.org/10.1016/j.cej.2012.05.051>.
- [39] A. Ghauch, A.M. Tuqan, N. Kibbi, S. Geryes, Methylene blue discoloration by heated persulfate in aqueous solution, *Chem. Eng. J.* 213 (2012) 259–271, <http://dx.doi.org/10.1016/j.cej.2012.09.122>.
- [40] A. Ghauch, A.M. Tuqan, N. Kibbi, Naproxen abatement by thermally activated persulfate in aqueous systems, *Chem. Eng. J.* 279 (2015) 861–873, <http://dx.doi.org/10.1016/j.cej.2015.05.067>.
- [41] A. Ghauch, G. Ayoub, S. Naim, Degradation of sulfamethoxazole by persulfate assisted micrometric Fe₀ in aqueous solution, *Chem. Eng. J.* 228 (2013) 1168–1181, <http://dx.doi.org/10.1016/j.cej.2013.05.045>.
- [42] S. Naim, A. Ghauch, Ranitidine abatement in chemically activated persulfate systems: assessment of industrial iron waste for sustainable applications, *Chem. Eng. J.* 288 (2016) 276–288.
- [43] M. Amasha, A. Baalbaki, S. Al Hakim, R. El Asmar, A. Ghauch, Degradation of a toxic molecule o-toluidine in industrial effluents using UV254/PS system, *J. Adv. Oxid. Technol.* 21 (2018).
- [44] A. Ghauch, A. Baalbaki, M. Amasha, R. El Asmar, O. Tantawi, Contribution of persulfate in UV-254nm activated systems for complete degradation of chloramphenicol antibiotic in water, *Chem. Eng. J.* 317 (2017) 1012–1025.
- [45] O.S. Furman, A.L. Teel, R.J. Watts, Mechanism of base activation of persulfate, *Environ. Sci. Technol.* 44 (2010) 6423–6428, <http://dx.doi.org/10.1021/es1013714>.
- [46] J. Kang, X. Duan, L. Zhou, H. Sun, M.O. Tadó, S. Wang, Carbocatalytic activation of persulfate for removal of antibiotics in water solutions, *Chem. Eng. J.* 288 (2016) 399–405.
- [47] C. Martínez, S. Vilarinho, M.I. Fernández, J. Faria, M. Canle L., J.A. Santaballa, Mechanism of degradation of ketoprofen by heterogeneous photocatalysis in

- aqueous solution, *Appl. Catal. B Environ.* 142–143 (2013) 633–646, <http://dx.doi.org/10.1016/j.apcatb.2013.05.018>.
- [48] A. Baalbaki, N.Z. Eddine, S. Jaber, M. Amasha, A. Ghauch, Rapid quantification of persulfate in aqueous systems using a modified HPLC unit, *Talanta* 178 (2018) 237–245.
- [49] M. Nie, Y. Yang, Z. Zhang, C. Yan, X. Wang, H. Li, W. Dong, Degradation of chloramphenicol by thermally activated persulfate in aqueous solution, *Chem. Eng. J.* 246 (2014) 373–382, <http://dx.doi.org/10.1016/j.cej.2014.02.047>.
- [50] Y. Fan, Y. Ji, D. Kong, J. Lu, Q. Zhou, Kinetic and mechanistic investigations of the degradation of sulfamethazine in heat-activated persulfate oxidation process, *J. Hazard. Mater.* 300 (2015) 39–47.
- [51] P. Neta, R.E. Huie, A.B. Ross, Rate constants for reactions of inorganic radicals in aqueous solution, *J. Phys. Chem. Ref. Data* 17 (1988) 1027–1284, <http://dx.doi.org/10.1063/1.555808>.
- [52] Y. Liu, X. He, Y. Fu, D.D. Dionysiou, Kinetics and mechanism investigation on the destruction of oxytetracycline by UV-254nm activation of persulfate, *J. Hazard. Mater.* 305 (2016) 229–239, <http://dx.doi.org/10.1016/j.jhazmat.2015.11.043>.
- [53] S.-Y. Oh, H.-W. Kim, J.-M. Park, H.-S. Park, C. Yoon, Oxidation of polyvinyl alcohol by persulfate activated with heat, Fe²⁺, and zero-valent iron, *J. Hazard. Mater.* 168 (2009) 346–351, <http://dx.doi.org/10.1016/j.jhazmat.2009.02.065>.
- [54] A. Ghauch, A.M. Tuqan, Oxidation of bisoprolol in heated persulfate/H₂O systems: kinetics and products, *Chem. Eng. J.* 183 (2012) 162–171, <http://dx.doi.org/10.1016/j.cej.2011.12.048>.
- [55] K.-C. Huang, R.A. Couttenye, G.E. Hoag, Kinetics of heat-assisted persulfate oxidation of methyl tert-butyl ether (MTBE), *Chemosphere* 49 (2002) 413–420.
- [56] J. Deng, Y. Shao, N. Gao, Y. Deng, S. Zhou, X. Hu, Thermally activated persulfate (TAP) oxidation of antiepileptic drug carbamazepine in water, *Chem. Eng. J.* 228 (2013) 765–771, <http://dx.doi.org/10.1016/j.cej.2013.05.044>.
- [57] C. Tan, N. Gao, Y. Deng, N. An, J. Deng, Heat-activated persulfate oxidation of diuron in water, *Chem. Eng. J.* 203 (2012) 294–300, <http://dx.doi.org/10.1016/j.cej.2012.07.005>.
- [58] P.A. MacFaul, L. Ruston, J.M. Wood, Activation energies for the decomposition of pharmaceuticals and their application to predicting hydrolytic stability in drug discovery, *Med. Chem. Commun.* 2 (2011) 140–142, <http://dx.doi.org/10.1039/C0MD00214C>.
- [59] H. Gao, J. Chen, Y. Zhang, X. Zhou, Sulfate radicals induced degradation of Triclosan in thermally activated persulfate system, *Chem. Eng. J.* 306 (2016) 522–530, <http://dx.doi.org/10.1016/j.cej.2016.07.080>.
- [60] Y.F. Rao, L. Qu, H. Yang, W. Chu, Degradation of carbamazepine by Fe(II)-activated persulfate process, *J. Hazard. Mater.* 268 (2014) 23–32, <http://dx.doi.org/10.1016/j.jhazmat.2014.01.010>.
- [61] A. Long, Y. Lei, H. Zhang, Degradation of toluene by a selective ferrous ion activated persulfate oxidation process, *Ind. Eng. Chem. Res.* 53 (2014) 1033–1039, <http://dx.doi.org/10.1021/ie402633n>.
- [62] A.K. Mitra, M.L. Matthews, Effects of pH and phosphate on the oxidation of iron in aqueous solution, *Int. J. Pharm.* 23 (1985) 185–193.
- [63] A. Ghauch, Rapid removal of flutriaol in water by zero-valent iron powder, *Chemosphere* 71 (2008) 816–826, <http://dx.doi.org/10.1016/j.chemosphere.2007.11.057>.
- [64] A. Tsitonaki, B. Petri, M. Crimi, H. Mosbæk, R.L. Siegrist, P.L. Bjerg, In situ chemical oxidation of contaminated soil and groundwater using persulfate: a review, *Crit. Rev. Environ. Sci. Technol.* 40 (2010) 55–91, <http://dx.doi.org/10.1080/10643380802039303>.
- [65] B.G. Petri, R.J. Watts, A. Tsitonaki, M. Crimi, N.R. Thomson, A.L. Teel, Fundamentals of ISCO using persulfate, *Situ Chem. Oxid. Groundw. Remediat.* Springer, 2011, pp. 147–191.
- [66] S. Norzaee, E. Bazrafshan, B. Djahed, F. Kord Mostafapour, R. Khaksefidi, UV activation of persulfate for removal of penicillin G antibiotics in aqueous solution, *Sci. World J.* 2017 (2017) 3519487, <http://dx.doi.org/10.1155/2017/3519487>.
- [67] M.A. Oturan, J.-J. Aaron, Advanced oxidation processes in water/wastewater treatment: principles and applications. A review, *Crit. Rev. Environ. Sci. Technol.* 44 (2014) 2577–2641.
- [68] H.A. Gorrell, Classification of formation waters based on sodium chloride content, *Am. Assoc. Pet. Geol. Bull.* 42 (1958) 2513.
- [69] Environment Protection Authority (EPA) in South Australia, Salinity, n.d.
- [70] C. Tan, D. Fu, N. Gao, Q. Qin, Y. Xu, H. Xiang, Kinetic degradation of chloramphenicol in water by UV/persulfate system, *J. Photochem. Photobiol. A Chem.* 332 (2017) 406–412, <http://dx.doi.org/10.1016/j.jphotochem.2016.09.021>.
- [71] L.R. Bennedson, J. Muff, E.G. Sogaard, Influence of chloride and carbonates on the reactivity of activated persulfate, *Chemosphere* 86 (2012) 1092–1097.
- [72] J. Deng, Y. Shao, N. Gao, S. Xia, C. Tan, S. Zhou, X. Hu, Degradation of the anti-epileptic drug carbamazepine upon different UV-based advanced oxidation processes in water, *Chem. Eng. J.* 222 (2013) 150–158, <http://dx.doi.org/10.1016/j.cej.2013.02.045>.
- [73] P.S. Hill, E.A. Schauble, E.D. Young, Effects of changing solution chemistry on Fe³⁺/Fe²⁺ isotope fractionation in aqueous Fe–Cl solutions, *Geochim. Cosmochim. Acta* 74 (2010) 6669–6689, <http://dx.doi.org/10.1016/j.gca.2010.08.038>.
- [74] V.P. Lemos, M.L. da Costa, R.L. Lemos, M.S.G. de Faria, Vivianite and siderite in lateritic iron crust: an example of bioreduction, *Quaternary* 11 (2007) 36–40.
- [75] S. Boggs, D. Livermore, M.G. Seitz, Humic substances in natural waters and their complexation with trace metals and radionuclides: a review, Argonne National Laboratory, 1985.
- [76] M.E. Lindsey, M.A. Tarr, Inhibited hydroxyl radical degradation of aromatic hydrocarbons in the presence of dissolved fulvic acid, *Water Res.* 34 (2000) 2385–2389.
- [77] Q. Zhang, J. Chen, C. Dai, Y. Zhang, X. Zhou, Degradation of carbamazepine and toxicity evaluation using the UV/persulfate process in aqueous solution, *J. Chem. Technol. Biotechnol.* 90 (2015) 701–708, <http://dx.doi.org/10.1002/jctb.4360>.
- [78] P.M.D. Gara, G.N. Bosio, M.C. Gonzalez, N. Russo, M. del Carmen Micheline, R.P. Diez, D.O. Mártire, A combined theoretical and experimental study on the oxidation of fulvic acid by the sulfate radical anion, *Photochem. Photobiol. Sci.* 8 (2009) 992–997.
- [79] P. Westerhoff, S.P. Mezyk, W.J. Cooper, D. Minakata, Electron pulse radiolysis determination of hydroxyl radical rate constants with suwannee river fulvic acid and other dissolved organic matter isolates, *Environ. Sci. Technol.* 41 (2007) 4640–4646, <http://dx.doi.org/10.1021/es062529n>.
- [80] C.S. Uyguner, M. Bekbolet, Evaluation of humic acid photocatalytic degradation by UV–vis and fluorescence spectroscopy, *Catal. Today* 101 (2005) 267–274.
- [81] B.M. Voelker, B. Sulzberger, Effects of fulvic acid on Fe (II) oxidation by hydrogen peroxide, *Environ. Sci. Technol.* 30 (1996) 1106–1114.
- [82] D. Vione, F. Merlo, V. Maurino, C. Minero, Effect of humic acids on the Fenton degradation of phenol, *Environ. Chem. Lett.* 2 (2004) 129–133.
- [83] A.L. Rose, T.D. Waite, Effect of dissolved natural organic matter on the kinetics of ferrous iron oxygenation in seawater, *Environ. Sci. Technol.* 37 (2003) 4877–4886.
- [84] J. Kochany, E. Lipczynska-Kochany, Fenton reaction in the presence of humates. Treatment of highly contaminated wastewater at neutral pH, *Environ. Technol.* 28 (2007) 1007–1013, <http://dx.doi.org/10.1080/09593332808618859>.
- [85] M.D. Paciolla, S. Kolla, S.A. Jansen, The reduction of dissolved iron species by humic acid and subsequent production of reactive oxygen species, *Adv. Environ. Res.* 7 (2002) 169–178, [http://dx.doi.org/10.1016/S1093-0191\(01\)00129-0](http://dx.doi.org/10.1016/S1093-0191(01)00129-0).
- [86] A. Georgi, A. Schierz, U. Trommler, C.P. Horwitz, T.J. Collins, F.-D. Kopinke, Humic acid modified Fenton reagent for enhancement of the working pH range, *Appl. Catal. B Environ.* 72 (2007) 26–36.
- [87] C. Fan, L. Tsui, M.-C. Liao, Parathion degradation and its intermediate formation by Fenton process in neutral environment, *Chemosphere* 82 (2011) 229–236, <http://dx.doi.org/10.1016/j.chemosphere.2010.10.016>.
- [88] S.-H. Kang, W. Choi, Oxidative degradation of organic compounds using zero-valent iron in the presence of natural organic matter serving as an electron shuttle, *Environ. Sci. Technol.* 43 (2009) 878–883, <http://dx.doi.org/10.1021/es801705f>.
- [89] B.K. Mayer, E. Daugherty, M. Abbaszadegan, Disinfection byproduct formation resulting from settled, filtered, and finished water treated by titanium dioxide photocatalysis, *Chemosphere* 117 (2014) 72–78.
- [90] L. Rizzo, A. Della Sala, A. Fiorentino, G.L. Puma, Disinfection of urban wastewater by solar driven and UV lamp – TiO₂ photocatalysis: effect on a multi drug resistant *Escherichia coli* strain, *Water Res.* 53 (2014) 145–152, <http://dx.doi.org/10.1016/j.watres.2014.01.020>.
- [91] G.P. Anipsitakis, T.P. Tufano, D.D. Dionysiou, Chemical and microbial decontamination of pool water using activated potassium peroxymonosulfate, *Water Res.* 42 (2008) 2899–2910.
- [92] X. He, A.A. de la Cruz, D.D. Dionysiou, Destruction of cyanobacterial toxin cylindrospermopsin by hydroxyl radicals and sulfate radicals using UV-254nm activation of hydrogen peroxide, persulfate and peroxymonosulfate, *J. Photochem. Photobiol. A Chem.* 251 (2013) 160–166, <http://dx.doi.org/10.1016/j.jphotochem.2012.09.017>.
- [93] K.A.K. Musa, J.M. Matxain, L.A. Eriksson, Mechanism of photoinduced decomposition of ketoprofen, *J. Med. Chem.* 50 (2007) 1735–1743, <http://dx.doi.org/10.1021/jm060697k>.
- [94] M.-D. Li, J. Ma, T. Su, M. Liu, L. Yu, D.L. Phillips, Direct observation of triplet state mediated decarboxylation of the neutral and anion forms of ketoprofen in water-rich, acidic, and PBS solutions, *J. Phys. Chem. B* 116 (2012) 5882–5887, <http://dx.doi.org/10.1021/jp301555e>.
- [95] J.R. Bolton, K.G. Bircher, W. Tumas, C.A. Tolman, Figures-of-merit for the technical development and application of advanced oxidation technologies for both electric and solar-driven systems (IUPAC Technical Report), *Pure Appl. Chem.* 73 (2001) 627–637.
- [96] J.A. Khan, X. He, N.S. Shah, H.M. Khan, E. Hapeshi, D. Fatta-Kassinos, D.D. Dionysiou, Kinetic and mechanism investigation on the photochemical degradation of atrazine with activated H₂O₂, S₂O₈²⁻ and HSO₅⁻, *Chem. Eng. J.* 252 (2014) 393–403, <http://dx.doi.org/10.1016/j.cej.2014.04.104>.